



Instrumentation of a geosynthetically reinforced roadway  
by Joseph Andrew Lapeyre

A thesis submitted in partial fulfillment of the requirements for the degree of Master of Science in Civil Engineering

Montana State University

© Copyright by Joseph Andrew Lapeyre (1996)

Abstract:

Reinforcing flexible pavement roadways with geosynthetics has been proposed to reduce the thickness of the base course layer. Mechanisms of reinforcement have been identified, but not quantified. A design procedure that incorporates the reinforcement provided by geosynthetics would provide more efficient use of aggregate and geosynthetics than those currently available. Research at Montana State University has been initiated in this area. Its goal is to quantify the reinforcing benefit of geosynthetics leading to the development of a roadway design procedure.

This thesis, which is the first phase of the research, is the study of possible strain sensors and installation techniques that can be used to monitor the performance of a geosynthetically reinforced roadway. With suitable strain sensors identified, the follow on phases of research at Montana State University will quantify the reinforcing benefit of geosynthetics.

Research was conducted in two areas. A full scale reinforced flexible pavement roadway was built and instrumented with vibrating wire, foil strain gauge, and LVDT technologies. The instruments were monitored over a four month period while the roadway was subjected to heavy truck traffic. The evaluation of mounting techniques used to fasten the strain sensors to the geosynthetics was accomplished with the use of a wide width uniaxial tension facility.

Results from the study show that all three of the technologies are viable candidates for use in further research. The effect of mounting techniques used to fasten the strain sensors to the geosynthetics was seen to have a major impact on the strain measured by the transducer. Calibration factors were developed to convert the strain measured by a sensor to the global strain in the geosynthetic. The need to account for temperature effects regarding thermal strain and signal distortion was also identified.

INSTRUMENTATION OF A GEOSYNTHETICALLY REINFORCED ROADWAY

by

Joseph Andrew Lapeyre

A thesis submitted in partial fulfillment  
of the requirements for the degree

of

Master of Science

in

Civil Engineering

MONTANA STATE UNIVERSITY  
Bozeman, Montana

December 1996

N378  
L3134

APPROVAL

of a thesis submitted by

Joseph Andrew Lapeyre

This thesis has been read by each member of the thesis committee and has been found to be satisfactory regarding content, English usage, format, citations, bibliographic style, and consistency, and is ready for submission to the College of Graduate Studies.

Dr. Steven W. Perkins

Steven W. Perkins  
(Signature)

12-2-96  
Date

Approved for the Department of Civil Engineering

Dr. Donald A. Rabern

Donald A. Rabern  
(Signature)

12/3/96  
Date

Approved for the College of Graduate Studies

Dr. Robert L. Brown

Robert L. Brown  
(Signature)

12/14/96  
Date

## STATEMENT OF PERMISSION TO USE

In presenting this thesis in partial fulfillment of the requirements for a master's degree at Montana State University-Bozeman, I agree that the Library shall make it available to borrowers under rules of the Library.

If I have indicated my intention to copyright this thesis by including a copyright notice page, copying is allowable only for scholarly purposes, consistent with "fair use" as prescribed in the U.S. Copyright Law. Requests for permission for extended quotation from or reproduction of this thesis in whole or in parts may be granted only by the copyright holder.

Signature

Joseph A. Lapeere

Date

9 Dec 96

## TABLE OF CONTENTS

	Page
1. INTRODUCTION .....	1
Background and Problem .....	1
Scope of Work .....	3
Outline of Thesis .....	4
2. LITERATURE REVIEW .....	5
Introduction .....	5
Strain Theory .....	5
Roadway Instrumentation .....	6
Strain Sensors for Cemented Material .....	7
H-Gauges .....	7
Foil Strain Gauges on Carrier Block .....	8
Foil Strain Gauges Mounted on Cores .....	9
Strain Gauges for Granular Material .....	10
Inductance Coils .....	10
LVDT's .....	11
Multidepth Deflectometers .....	11
Instrumented Roadways .....	14
Full Scale Tests .....	14
MN/ROAD .....	14
Center for Transportation Research, Univ of Texas .....	16
North Carolina Instrumented Highway .....	16
Alberta Instrumented Highway .....	17
TRRL Instrumented Highway .....	17
Laboratory Tests .....	18
Virginia Polytechnical Institute .....	18
Danish Road Testing Machine .....	19
U.S. Army Engineer Waterways Station .....	21
University of Waterloo .....	21
Tension Testing of Geosynthetics .....	22
Introduction .....	22
ASTM Standards .....	23
Laboratory Testing .....	24
Related Instrumented Geosynthetic Studies .....	27
3. RESEARCH METHODOLOGY .....	30
Introduction .....	30
Instrumented Roadway .....	30
Instrument types .....	30

	Page
Asphalt Concrete .....	30
Instrumentation in the Base Course .....	32
Instrumentation on the Geosynthetics .....	34
Data Logging Systems .....	38
Long Term Data Logger .....	39
Dynamic Data Logger .....	39
Roadway Monitoring .....	40
Long Term Monitoring Program .....	40
Dynamic Monitoring Program .....	41
Roadway Construction and Gauge Locations .....	45
Introduction .....	45
Roadway Construction Overview .....	46
Instrumentation Layout .....	47
Instrumentation Installation .....	50
Instruments Attached to the Geosynthetics .....	50
Instruments Embedded in Base Course .....	51
Instruments Embedded in Asphalt Concrete .....	53
Wide Width Tension Testing .....	54
Loading Frame .....	54
Sensors Used for Local Strain Measurement .....	58
Tests Performed .....	61
 4. RESULTS.....	 63
Introduction.....	63
Wide Width Tension Testing .....	63
Accuracy and Repeatability .....	63
Comparison of Global Strain to Manufacturer's Specifications ..	64
Strain Response of the Vibrating Wire Strain Gauges .....	64
Strain Response of the Vibrating Wire Displacement Gauges ..	66
Strain Response of the LVDT Gauges .....	68
Strain Response in the Foil Strain Gauges .....	68
Summary .....	70
Roadway Results .....	72
Long Term Results .....	72
Truck Traffic Loading .....	72
Strain in the Geosynthetics .....	72
Strain Gauges in the Base Course .....	76
Strain in the AC .....	78
Dynamic Testing Results .....	79
Truck Pass Tests .....	79
Road Rater Tests .....	81

	Page
5. CONCLUSIONS AND RECOMMENDATIONS .....	85
Conclusions .....	85
Recommendations .....	86
REFERENCES CITED .....	89
APPENDICES .....	92
A Wide Width Tension Testing Results .....	93
B Roadway Results .....	116

## LIST OF TABLES

Table	Page
1. Chronological Order of Events For Roadway Construction and Testing .....	42
2. Vehicles Used for Truck Pass Tests .....	44
3. Instrumentation Specifications .....	50
4. Geosynthetic Instrument Cover Options .....	52

## LIST OF FIGURES

Figure	Page
1. Dynatest H-Gauge .....	8
2. Foil Strain Gauge mounted in a Carrier Block .....	9
3. LVDT .....	12
4. Cross section of MDD after installation .....	13
5. The Danish Road Testing Machine .....	20
6. ASTM approved Sanders Clamp .....	25
7. ASTM approved Wide Width Clamp .....	26
8. Vibrating Wire Embedment AC Strain Gage (Geokon Model VCE-4200-HT) .....	31
9. Vibrating Wire Embedment Strain Gage (Geokon Model VCE-4200) .....	32
10. Vibrating Wire Embedment Displacement Gage (Geokon Model 4430) .....	33
11. LVDT Embedment Displacement Gage (RDP Electronics Model D5/400W) .....	34
12. Vibrating Wire Strain Gage (Geokon Model VSM-4000) .....	35
13. Vibrating Wire Displacement Gage (Geokon Model 4420) .....	36
14. LVDT Displacement Gage (RDP Electronics Model D5/200W) .....	37
15. Plan View of Roadway Test Sight .....	48
16. Roadway Instrumentation Layout .....	49

Figure	Page
17. Schematic of Wide Width Tension Testing Frame .....	56
18. Dimensional Placement of Instruments on a Geosynthetic Specimen ...	60
19. Global Strain From Two Sets of Celesco Gages: Geogrid, Machine Direction .....	94
20. Global Strain From Two Sets of Celesco Gages: Geogrid, Transverse Direction .....	94
21. Global Strain From Two Sets of Celesco Gages: Geotextile, Machine Direction .....	95
22. Global Strain From Two Sets of Celesco Gages: Geotextile, Transverse Direction .....	95
23. Global Strain From Two Tests: Geogrid, Machine Direction .....	96
24. Global Strain From Two Tests: Geogrid, Transverse Direction .....	96
25. Global Strain From Two Tests: Geotextile, Machine Direction .....	97
26. Global Strain From Two Tests: Geotextile, Transverse Direction .....	97
27. Comparison of Results to Manufacturer's Data: Geogrid, Machine Direction .....	98
28. Comparison of Results to Manufacturer's Data: Geogrid, Transverse Direction .....	98
29. Comparison of Results to Manufacturer's Data: Geotextile, Machine Direction .....	99
30. Comparison of Results to Manufacturer's Data: Geotextile, Transverse Direction .....	99

Figure	Page
31. Vibrating Wire Strain Gage: Geogrid, Machine Direction .....	100
32. Vibrating Wire Strain Gage: Geogrid, Transverse Direction .....	100
33. Vibrating Wire Strain Gage: Geotextile, Machine Direction .....	101
34. Vibrating Wire Strain Gage: Geotextile, Transverse Direction .....	101
35. Calibrated Vibrating Wire Strain Gage: Geogrid, Machine Direction .....	102
36. Calibrated Vibrating Wire Strain Gage: Geogrid, Transverse Direction .....	102
37. Calibrated Vibrating Wire Strain Gage: Geotextile, Machine Direction .....	103
38. Calibrated Vibrating Wire Strain Gage: Geotextile, Transverse Direction .....	103
39. Comparison of Vibrating Wire Strain Gage With 6, 4 and 2 Bolts Fastened .....	104
40. Vibrating Wire Displacement Gage: Geogrid, Machine Direction .....	104
41. Vibrating Wire Displacement Gage: Geogrid, Transverse Direction .....	105
42. Vibrating Wire Displacement Gage: Geotextile, Machine Direction .....	105
43. Vibrating Wire Displacement Gage: Geotextile, Transverse Direction .....	106
44. Calibrated Back-to-Back Vibrating Wire Displacement Gage: Geogrid, Machine Direction .....	106

Figure	Page
45. Calibrated Back-to-Back Vibrating Wire Displacement Gage: Geogrid, Transverse Direction .....	107
46. Calibrated Back-to-Back Vibrating Wire Displacement Gage: Geotextile, Machine Direction .....	107
47. Calibrated Back-to-Back Vibrating Wire Displacement Gage: Geotextile, Transverse Direction .....	108
48. LVDT Displacement Gage: Geogrid, Machine Direction .....	108
49. LVDT Displacement Gage: Geogrid, Transverse Direction .....	109
50. LVDT Displacement Gage: Geotextile, Machine Direction .....	109
51. LVDT Displacement Gage: Geotextile, Transverse Direction .....	110
52. Calibrated LVDT Displacement Gage: Geogrid, Machine Direction .....	110
53. Calibrated LVDT Displacement Gage: Geotextile, Machine Direction .....	111
54. Calibrated LVDT Displacement Gage: Geotextile, Transverse Direction .....	111
55. Foil Strain Gage: Geogrid, Machine Direction .....	112
56. Foil Strain Gage: Geogrid, Transverse Direction .....	112
57. Calibrated Foil Strain Gage: Geogrid, Machine Direction .....	113
58. Calibrated Foil Strain Gage: Geogrid, Transverse Direction .....	113
59. Unloading-Reloading Response From Foil Strain Gage: Geogrid, Transverse Direction .....	114
60. Calibrated 1/4 Bridge Foil Strain Gage: Geogrid, Machine Direction .....	114

Figure	Page
61. Calibrated Foil Strain Gage With Environmental Protection: Geogrid, Machine Direction .....	115
62. Calibrated Foil Strain Gage With Environmental Protection: Geogrid, Transverse Direction .....	115
63. Daily Traffic Loading History .....	117
64. Weekly Truck Traffic Loading History .....	117
65. VW Displacement Gage #2 on Geogrid (on wheel-path) .....	118
66. VW Displacement Gage #1 on Geotextile (off wheel-path) .....	118
67. VW Strain Gage #6 on Geogrid (off wheel-path) .....	119
68. VW Strain Gage #5 on Geotextile (on wheel-path) .....	119
69. LVDT Displacement Gage #31 on Geogrid (on wheel-path) .....	120
70. LVDT Displacement Gage #32 on Geogrid (off wheel-path) .....	121
71. LVDT Displacement Gage #29 on Geotextile (on wheel-path) .....	122
72. LVDT Displacement Gage #30 on Geotextile (off wheel-path) .....	123
73. VW Embedment Displacement Gage #3 in Base Above Geogrid (off wheel-path) .....	124
74. VW Embedment Displacement Gage #4 in Base in Non-Reinforced Section (on wheel-path) .....	124
75. VW Embedment Strain Gage #8 in Base Above Geogrid (on wheel-path) .....	125
76. VW Embedment Strain Gage #7 in Base Above Geotextile (on wheel-path) .....	125

Figure	Page
77. LVDT Embedment Displacement Gage #27 in Base Above Geogrid (off wheel-path) .....	126
78. LVDT Embedment Displacement Gage #28 in Base Above Geogrid (on wheel-path) .....	127
79. LVDT Embedment Displacement Gage #25 in Base Above Geotextile (on wheel-path) .....	128
80. LVDT Embedment Displacement Gage #26 in Base in Non-Reinforced Section (on wheel-path) .....	129
81. VW Embedment Strain Gage #10 in AC Above Geogrid (on wheel-path) .....	130
82. VW Embedment Strain Gage #11 in AC Above Geogrid (off wheel-path) .....	131
83. VW Embedment Strain Gage #9 in AC Above Geotextile (on wheel-path) .....	132
84. VW Embedment Strain Gage #12 in AC in Non-Reinforced Section (on wheel-path) .....	133
85. Foil Strain Gage #36 on Geogrid (on wheel path): Truck Pass Test 1 .....	134
86. Foil Strain Gage #35 on Geogrid (below centerline): Truck Pass Test 1 .....	134
87. Foil Strain Gage #36 on Geogrid (on wheel path): Truck Pass Test 2 .....	135
88. Foil Strain Gage #35 on Geogrid (below centerline): Truck Pass Test 2 .....	135
89. Foil Strain Gage #36 on Geogrid (on wheel path): Truck Pass Test 3 .....	136
90. Foil Strain Gage #35 on Geogrid (below centerline): Truck Pass Test 3 .....	136

Figure	Page
91. Foil Strain Gage #34 on Geogrid (on wheel path): Truck Pass Test 3 .....	137
92. Foil Strain Gage #36 on Geogrid (on wheel path): Truck Pass Test 4 .....	137
93. Foil Strain Gage #35 on Geogrid (below centerline): Truck Pass Test 4 .....	138
94. Foil Strain Gage #34 on Geogrid (on wheel path): Truck Pass Test 4 .....	138
95. Foil Strain Gage #36 on Geogrid (on wheel path): Truck Pass Test 5 .....	139
96. Foil Strain Gage #35 on Geogrid (below centerline): Truck Pass Test 5 .....	139
97. Foil Strain Gage #34 on Geogrid (on wheel path): Truck Pass Test 5 .....	140
98. Foil Strain Gage #36 on Geogrid (on wheel path): Truck Pass Test 6 .....	140
99. Foil Strain Gage #35 on Geogrid (below centerline): Truck Pass Test 6 .....	141
100. Foil Strain Gage #34 on Geogrid (on wheel path): Truck Pass Test 6 .....	141
101. Foil Strain Gage #36 on Geogrid (on wheel path): Truck Pass Test 7 .....	142
102. Foil Strain Gage #35 on Geogrid (below centerline): Truck Pass Test 7 .....	142
103. Foil Strain Gage #34 on Geogrid (on wheel path): Truck Pass Test 7 .....	143
104. Foil Strain Gage #36 on Geogrid (on wheel path): Truck Pass Test 8 .....	143

Figure	Page
105. Foil Strain Gage #35 on Geogrid (below centerline): Truck Pass Test 8 .....	144
106. Foil Strain Gage #36 on Geogrid (on wheel path): Truck Pass Test 9 .....	144
107. Foil Strain Gage #35 on Geogrid (below centerline): Truck Pass Test 9 .....	145
108. LVDT Displacement Gage #31 on Geogrid (on wheel path): Truck Pass Test 4 .....	145
109. LVDT Displacement Gage #31 on Geogrid (on wheel path): Truck Pass Test 5 .....	146
110. LVDT Displacement Gage #32 on Geogrid (off wheel path): Truck Pass Test 5 .....	146
111. LVDT Displacement Gage #29 on Geotextile (on wheel path): Truck Pass Test 4 .....	147
112. LVDT Displacement Gage #29 on Geotextile (on wheel path): Truck Pass Test 5 .....	147
113. LVDT Displacement Gage #29 on Geotextile (on wheel path): Truck Pass Test 6 .....	148
114. LVDT Embedment Displacement Gage #27 in Base Above Geogrid (off wheel path): Truck Pass Test 3 .....	148
115. LVDT Embedment Displacement Gage #27 in Base Above Geogrid (off wheel path): Truck Pass Test 6 .....	149
116. LVDT Embedment Displacement Gage #27 in Base Above Geogrid (off wheel path): Truck Pass Test 7 .....	149
117. LVDT Embedment Displacement Gage #28 in Base Above Geogrid (on wheel path): Truck Pass Test 2 .....	150
118. LVDT Embedment Displacement Gage #28 in Base Above Geogrid (on wheel path): Truck Pass Test 3 .....	150

Figure	Page
119. LVDT Embedment Displacement Gage #28 in Base Above Geogrid (on wheel path): Truck Pass Test 4 .....	151
120. LVDT Embedment Displacement Gage #28 in Base Above Geogrid (on wheel path): Truck Pass Test 5 .....	151
121. LVDT Embedment Displacement Gage #28 in Base Above Geogrid (on wheel path): Truck Pass Test 6 .....	152
122. LVDT Embedment Displacement Gage #25 in Base Above Geotextile (on wheel path): Truck Pass Test 1 .....	152
123. LVDT Embedment Displacement Gage #25 in Base Above Geotextile (on wheel path): Truck Pass Test 2 .....	153
124. LVDT Embedment Displacement Gage #25 in Base Above Geotextile (on wheel path): Truck Pass Test 3 .....	153
125. LVDT Embedment Displacement Gage #25 in Base Above Geotextile (on wheel path): Truck Pass Test 4 .....	154
126. LVDT Embedment Displacement Gage #25 in Base Above Geotextile (on wheel path): Truck Pass Test 5 .....	154
127. LVDT Embedment Displacement Gage #25 in Base Above Geotextile (on wheel path): Truck Pass Test 6 .....	155
128. LVDT Embedment Displacement Gage #25 in Base Above Geotextile (on wheel path): Truck Pass Test 7 .....	155
129. LVDT Embedment Displacement Gage #26 in Base of Non-Reinforced Section (on wheel path): Truck Pass Test 1 ...	156
130. LVDT Embedment Displacement Gage #26 in Base of Non-Reinforced Section (on wheel path): Truck Pass Test 2 ...	156
131. LVDT Embedment Displacement Gage #26 in Base of Non-Reinforced Section (on wheel path): Truck Pass Test 3 ...	157
132. LVDT Embedment Displacement Gage #26 in Base of Non-Reinforced Section (on wheel path): Truck Pass Test 4 ...	157

Figure	Page
133. LVDT Embedment Displacement Gage #26 in Base of Non-Reinforced Section (on wheel path): Truck Pass Test 5 . . .	158
134. LVDT Embedment Displacement Gage #26 in Base of Non-Reinforced Section (on wheel path): Truck Pass Test 6 . . .	158
135. Foil Strain Gage #34 on Geogrid, July 31st Test . . . . .	159
136. Foil Strain Gage #35 on Geogrid, July 31st Test . . . . .	159
137. Foil Strain Gage #36 on Geogrid, July 31st Test . . . . .	160
138. Foil Strain Gage #34 on Geogrid, September 21st Test . . . . .	160
139. Foil Strain Gage #35 on Geogrid, September 21st Test . . . . .	161
140. Foil Strain Gage #36 on Geogrid, September 21st Test . . . . .	161
141. VW Displacement Gage #2 on Geogrid, September 21st Test . . . . .	162
142. VW Strain Gage #5 on Geotextile, September 21st Test . . . . .	162
143. VW Embedment Displacement Gage #3 in Base Above Geogrid, September 21st Test . . . . .	163
144. VW Embedment Strain Gage #7 in Base Above Geotextile, September 21st Test . . . . .	163
145. VW Embedment Strain Gage #9 in AC Above Geotextile, September 21st Test . . . . .	164
146. Resilient Modulus Values From July 21 Road Rater Test . . . . .	164
147. Average Resilient Modulus Values From July 21 Road Rater Test . . . . .	165
148. Resilient Modulus of AC Layer From September 21 Road Rater Test . . . . .	165
149. Resilient Modulus of Base and Subgrade Layers From September 21 Road Rater Test . . . . .	166

Figure	Page
150. Average Resilient Modulus of AC Layer From September 21 Road Rater Test .....	166
151. Average Resilient Modulus of Base and Subgrade Layers From September 21 Road Rater Test .....	167

## ABSTRACT

Reinforcing flexible pavement roadways with geosynthetics has been proposed to reduce the thickness of the base course layer. Mechanisms of reinforcement have been identified, but not quantified. A design procedure that incorporates the reinforcement provided by geosynthetics would provide more efficient use of aggregate and geosynthetics than those currently available. Research at Montana State University has been initiated in this area. Its goal is to quantify the reinforcing benefit of geosynthetics leading to the development of a roadway design procedure.

This thesis, which is the first phase of the research, is the study of possible strain sensors and installation techniques that can be used to monitor the performance of a geosynthetically reinforced roadway. With suitable strain sensors identified, the follow on phases of research at Montana State University will quantify the reinforcing benefit of geosynthetics.

Research was conducted in two areas. A full scale reinforced flexible pavement roadway was built and instrumented with vibrating wire, foil strain gauge, and LVDT technologies. The instruments were monitored over a four month period while the roadway was subjected to heavy truck traffic. The evaluation of mounting techniques used to fasten the strain sensors to the geosynthetics was accomplished with the use of a wide width uniaxial tension facility.

Results from the study show that all three of the technologies are viable candidates for use in further research. The effect of mounting techniques used to fasten the strain sensors to the geosynthetics was seen to have a major impact on the strain measured by the transducer. Calibration factors were developed to convert the strain measured by a sensor to the global strain in the geosynthetic. The need to account for temperature effects regarding thermal strain and signal distortion was also identified.

## CHAPTER 1

## INTRODUCTION

Background and Problem

The use of geosynthetics (geotextiles and geogrids) has become prevalent in geotechnical and transportation projects in recent years. It has been proposed that it may be possible to reinforce the base course layer in paved roadways with geosynthetics. If true, this would be of great benefit in certain projects. Some areas, such as Eastern Montana, have limited natural sources of quality aggregate for base course construction. It often is cost prohibitive to transport aggregate to these areas. For these areas, reducing base course thickness with reinforcement through the use of geosynthetics may be a cost effective alternative to bringing in outside aggregate.

Currently, the improvement in performance gained by adding geosynthetics to the base layer reinforcement is poorly understood. Studies have shown conflicting results with regard to geosynthetic reinforcement of base courses in paved roadways. This situation is partially due to the lack of understanding of the mechanical performance of geosynthetically reinforced roadways. Research at Montana State University has been initiated in this area with the goal of describing the reinforcement performance of geosynthetics in paved roadways and providing a design tool for geosynthetically reinforced flexible pavements.

The research program at Montana State University involves several areas of study. To examine the interaction between geosynthetics and base course, a confined geosynthetic

pullout facility has been constructed. The facility is a 6 walled steel box in which a geosynthetic is sandwiched in base material. An air bladder provides confining pressure to the top of the base course material. Once the desired level of confinement is achieved, the geosynthetic is pulled through the box by means of a low geared electric motor. Strain instrumentation on the geosynthetic and a load cell in the pull out mechanism provides measurements of the geosynthetic performance. In addition to providing information on the interaction between the geosynthetic and base course, creep and stress relaxation effects in geosynthetic may be studied.

To identify conditions under which geosynthetic reinforcement is seen to offer improvement, a cyclic load plate facility is being constructed. This facility is a reinforced concrete box in which a roadway structure is built and instrumented. A pneumatically activated circular plate mounted on a steel H beam is used to apply loads to the roadway. Through the use of rollers, the steel plate will be able to move over the surface of the roadway to apply the load at specific locations. The performance of the roadway structure will help identify types of test sections that are necessary to advance the understanding of geosynthetic reinforcement.

With knowledge gained from the two laboratory tests a design procedure will be established. Finite element analysis will be important in developing the design procedure. A finite element model of the cyclic load plate facility will be created and verified against the measured performance. The model will then be used to develop the design procedure. Once the design procedure is established, it will be verified by constructing a full scale test road.

To study the mechanisms of reinforcement in a geosynthetically reinforced roadway the mechanical performance of the roadway must be measured. Parameters such as stress, strain, pore water pressure, moisture content, and temperature need to be measured at select locations in the roadway cross section. For many geotechnical structures involving only granular materials and long term static loading, measurement of these parameters is well established. For geosynthetics and roadway studies however, the methodology is not as clearly established. In addition to the granular base course of the roadway, measurements need to be made in the asphalt concrete (AC) pavement, and on the geosynthetic. Long term measurements as well as short term dynamic responses from individual axle loadings need to be made. During the initial research at Montana State University, particular concerns existed regarding strain measurements. The appropriate strain gauges for use in roadways and attendant installation techniques had to be determined before the research could continue. Therefore the topic of this study is examination of the proposed strain measuring instrumentation and installation techniques for use in follow on research.

#### Scope of Work

The study consists of two areas. First, a fully instrumented geosynthetic reinforced roadway was constructed and monitored. The roadway study provided information in two areas. Gauge performance, including both strain measurement and reliability was evaluated. Second, installation techniques for the strain gauges were evaluated. The roadway carried over 7000 passes of heavy truck traffic during its 4 month life. It consisted of a geogrid reinforced section, a geotextile reinforced section, and a control section. The roadway

contained a total of 24 strain gauges located in the AC, base course, and mounted on the geosynthetics. Two types of strain measurements were made. Static long term cumulative strain measurements were recorded over the life time of the roadway as well as dynamic short term measurements of specific events, such as the loading from a single axle.

To support the in-field study, a wide width tension testing facility was constructed in the laboratory. This facility was used to study the strain gauges mounted on the geosynthetics. The facility was able to test geosynthetic specimens up to 1.83 m wide and 3 m long. Tests in the facility covered three objectives. First, it allowed comparison of the local strain in a geosynthetic (measured by a strain gauge) to the global strain experienced by the geosynthetic when subjected to a uniaxial load. Second, the mounting techniques used for the strain gauges in the field were evaluated. Third, the stress strain response of the geosynthetic provided by the manufacturer was verified.

#### Outline of the Thesis

The thesis is organized into 5 chapters. Chapter 2 is a literature review to provide background information concerning instrumentation of roadways and geosynthetics. Its main topics are strain gauge types, previous instrumented roadway studies, and tension testing of geosynthetics. Chapter 3 provides a detailed discussion of the experimental work performed by the author. Topics include instrumentation used in the study, roadway construction, and the wide width tension testing facility. Chapter 4 provides results of the study. Chapter 5 is devoted to conclusions and recommendations for further work.

## CHAPTER 2

## LITERATURE REVIEW

Introduction

The literature review consists of five sections. In section one, a brief presentation of the calculation of strain is made. Section two presents the types of strain sensors used in roadway studies. Previous instrumented roadway studies from both the field and laboratory are discussed in section three. Section four looks at the ASTM tension test for geosynthetics and the significant parameters for tension tests in general. Section five discusses other geosynthetic instrumented projects with regards to bonding foil strain gauges to geogrids.

Strain Theory

Strain ( $\epsilon$ ) is a measurement of the relative change in length of an object. It is defined as the ratio of the change in length ( $\delta L$ ) of an object to its original length ( $L$ ). This relationship can be written as:

$$\epsilon = \frac{\delta L}{L} \quad (1)$$

The relationship of the strain of an object to the force causing the strain is in general non-linear. For many engineering situations however, the magnitude of the strains is small, covering only the linear portion of the material's stress-strain diagram. Hooke's Law governs the stress-strain relationship of a material in this region. It states that the stress is

directly proportional to the strain. It is written as the following:

$$\sigma = \epsilon E \quad (2)$$

The importance of this relationship is that it allows the calculation of stress ( $\sigma$ ) based on the measured strain and the material property  $E$ , the modulus of elasticity.

Several technologies are used to measure strain. Electrical and mechanical are most common but optical, acoustical, and pneumatic strain sensors exist. Regardless of the phenomena, all strain gauges rely on the measurement of the displacement between two points a known distance apart and then the computation of strain using equation 1.

#### Roadway Instrumentation

Due to the different materials in a roadway structure, there are several types of strain sensors typically used. In granular material the technology used is different from that used in cemented material such as AC or concrete. The profile of a strain sensor for granular material is large in order to produce an accurate measurement. Strain sensors in cemented material do not always have this luxury due to the small thickness of the surface material. Additionally, the installation of strain sensors in cemented material typically occurs when the hot mix is placed. This requires high temperature resistance of both the instrument and its electrical cables.

## Strain Sensors for Cemented Material

H-Gauges. H-gauges are given their name from their appearance (See figure 1). They consist of a strip of material onto which a foil strain gauge is bonded. On each end of the strip, metal bars are fixed at their midpoint. The metal bars serve as anchors in the cemented material. Thus when the material is strained the metal bars move relative to each other and the resulting strain in the strip material is measured by the foil strain gauge. The length of the gauge should depend on the size of the aggregate in the AC. For pavement materials it is commonly believed that the gauge length should be at least 4 to 5 times the maximum particle diameter (Van Deusen, 1992). To ensure that accurate strain readings are being made it is important that the stiffness of the strip be the same or less than that of the cemented material. If it is greater, the H-gauge will under measure the actual strain of the cemented material.

The first H-gauges were designed by the Transportation Road Research Laboratory (TRRL) in Great Britain (Sebaaly, 1989). Important aspects of their evolution include better matching of gauge and material stiffnesses, and survivability of the foil strain gauge. To this end current H-gauges manufactured by Dynatest Corporation use epoxy reinforced fiberglass as the strip material (Van Deusen, 1992). Fiberglass has the desired properties of low stiffness and high flexibility. To increase survivability, the foil strain gauge is embedded in the fiberglass. Additionally, various layers of waterproofing compounds and aluminum plates are placed around the fiberglass strip.

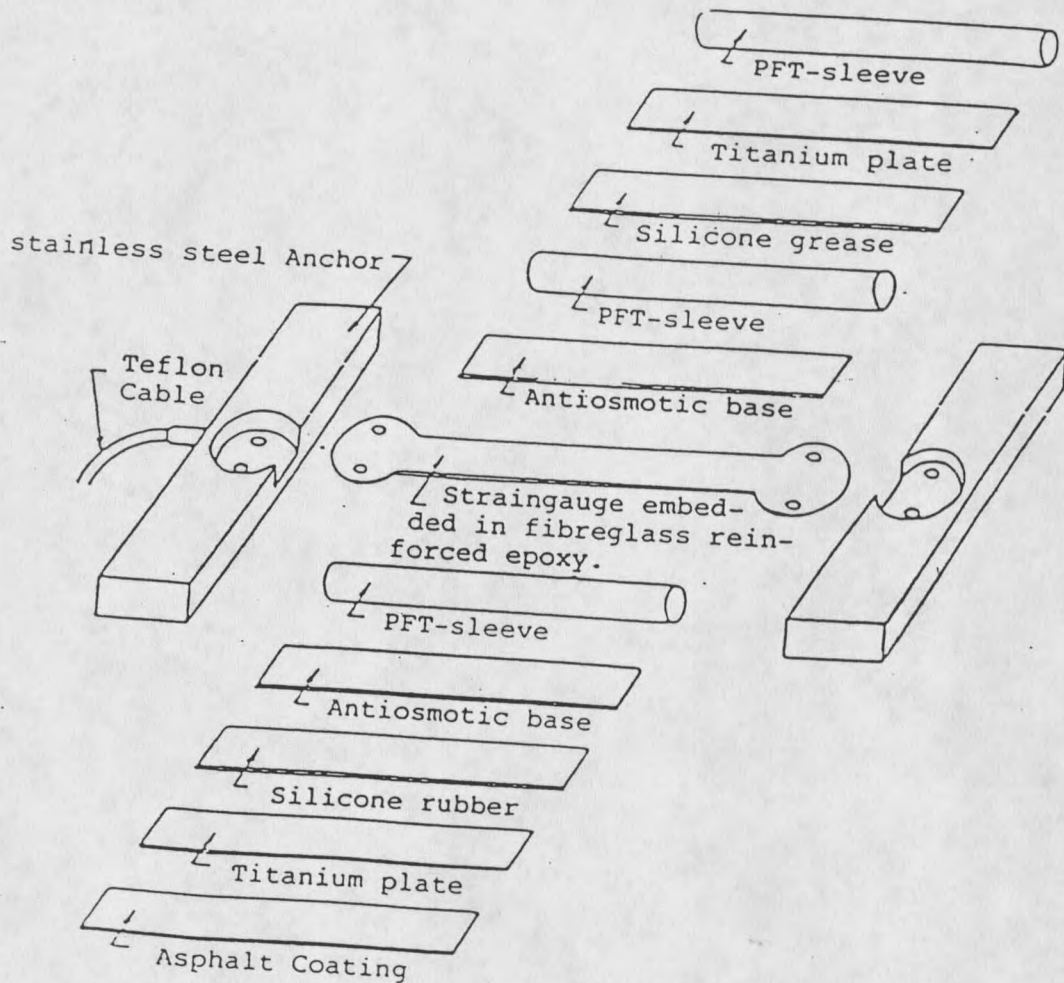


Figure 1. Dynatest H-Gauge (from Van Deusen et al., 1992)

Foil Strain Gauges on Carrier Block. Carrier blocks are laboratory compacted AC bricks to which foil strain gauges have been attached. When the hot mix lift is being constructed, the carrier block is placed on the base course in the proper location and orientation. As the hot mix surrounds the carrier block the heat softens the carrier block and the hot mix and carrier block bond forming a monolithic layer of AC.

A drawback of carrier blocks is protection of the foil strain gauge when the hot mix softens the block. Debonding and mechanical damage of the gauge are possible. A technique to overcome this dilemma is to cut the carrier block in the lab and mount the foil strain gauge on the cut surface as seen in figure 2. The carrier block is then glued back together. The location of the foil strain gauge in the middle of the carrier block gives it protection from aggregate in the hot mix. The location also minimizes temperature change around the gauge, which can be detrimental to the bonding agent.

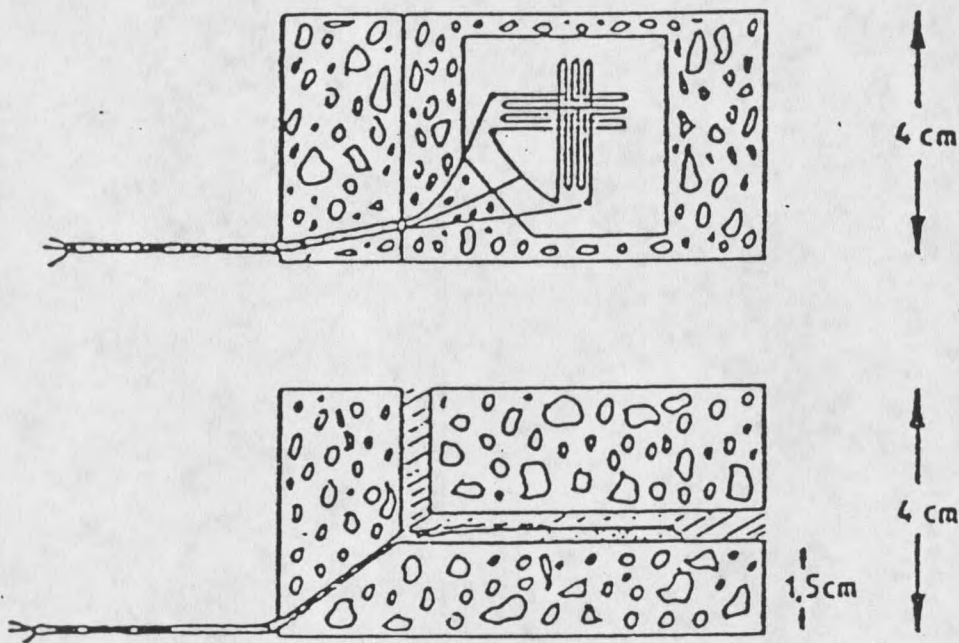


Figure 2. Foil Strain Gauge mounted in a Carrier Block (from Sebaaly et al., 1989)

Foil Strain Gauges Mounted on Cores. This technique is similar to a carrier block except that the core is cut out of the existing roadway. Bonding the core back to the AC is a significant problem. The stiffness of the bonding agent and that of the AC must be closely

matched. If the bonding agent is soft relative to the AC the core tends to act as a rigid body immersed in a monolithic material. If the bonding agent is stiff relative to the AC, stress concentrations will occur in the core, which induce cracking and premature failure of the core. A major advantage of using cores is that the instruments can be easily placed after the roadway is constructed.

### Strain Gauges for Granular Material

Inductance Coils. Inductance coils are two disc shaped coils that produce an electromagnetic output proportional to the distance between them. They are available commercially from Bison Instruments, Inc. The discs may be oriented coplanar, orthogonal, or most commonly coaxial. Typical distance between the disks is 1 to 4 times the diameter of a single disk (Selig, 1975). One of the disks acts as a transmitter and the other as a receiver. As the distance between them changes, the response of the coil in the receiver changes which is converted to a displacement. Inductance coils have a unique advantage in that the two discs are not mechanically connected. Therefore disturbance and altering of the tested material is not an issue. They have good stability for long term measurements, but are subject to error when used for certain dynamic measurements. Poor performance in dynamic measurements can be caused by the movement of the vehicle applying the load through the gauge's electromagnetic field. The metal and electrical system of the vehicle induces changes in the field of the gauge. The strain resolution for long-term and dynamic measurements is 0.003 % and 0.1 % respectively (Brown, 1977). Inductance coils appear to have excellent durability. Selig (1975) notes a roadway study in which less than 1% of

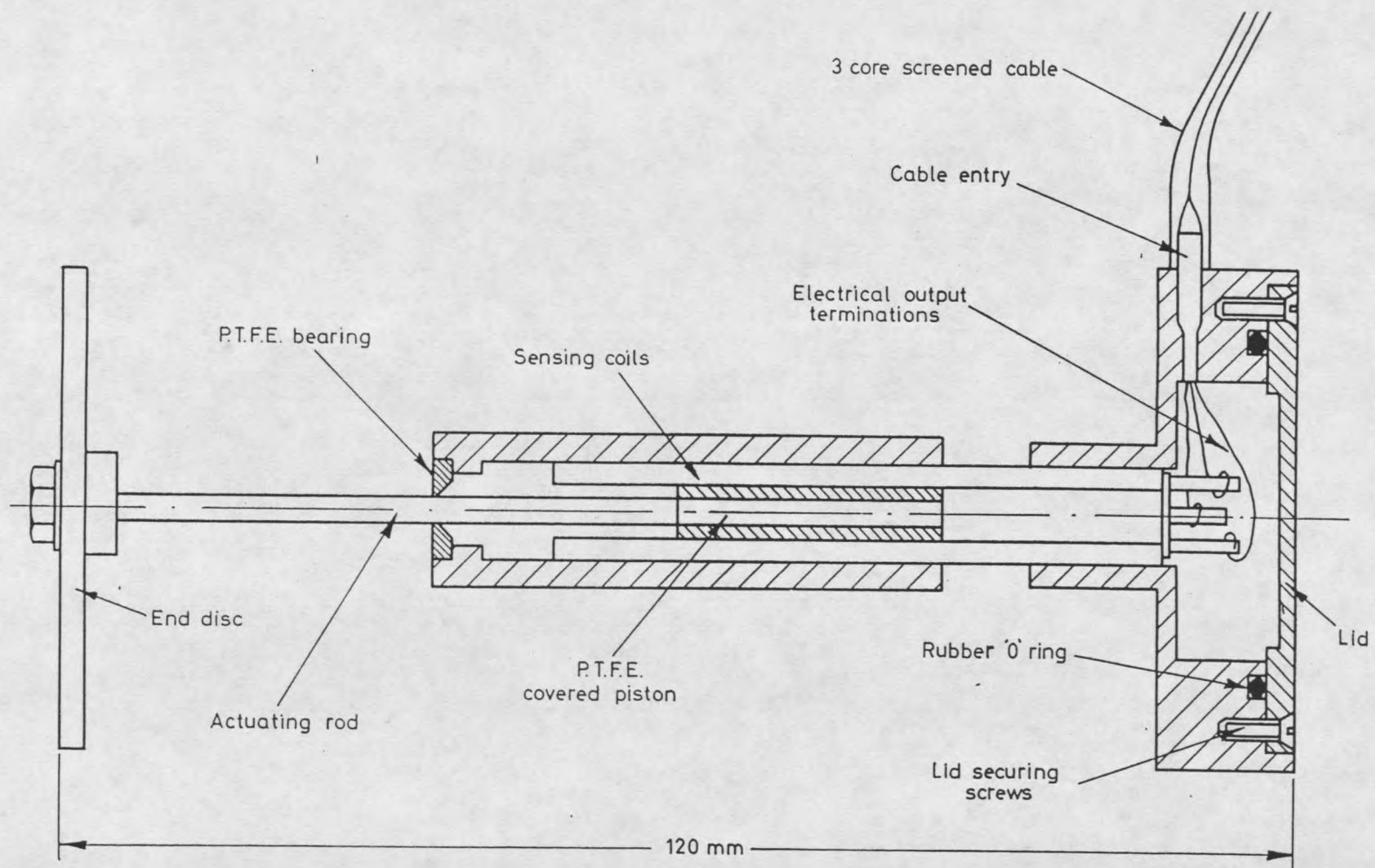
408 gauges were inoperative after one year in service.

LVDT. Linear Variable Differential Transformers (LVDT) use electro-mechanical effects to measure displacement. The gauge operates by moving a rod shaped core through a cylinder containing three symmetrically spaced electrical coils. The center coil, called the primary coil, creates an electrical field with power from an external source. As the core moves through the electrical field it provides a pathway for magnetic flux to induce a voltage in the two secondary coils. The induced voltages are directly proportional to the position of the core allowing displacement and subsequent strain measurements to be made.

A typical LVDT is shown in figure 3. The gauges are composed of a rod shaped core with an attached disk and a cylinder with a similar attached disk. As the granular material shifts, the discs are forced to move which causes displacement of the core relative to the coils.

LVDT's are available in both DC and AC models. AC models are more common in situations where environmental protection is an issue because the electronic circuitry can be housed separate from the gauge. Separating the electronics from the gauge also allows a physically smaller unit to be used.

Multidepth Deflectometer. Multidepth deflectometers (MDD) are a series of connected LVDTs used to measure deflections at various depths in a roadway structure (Pilson, 1995). A roadway cross section instrumented with an MDD is shown in figure 4.



12

Figure 3. LVDT (from Potter et al, 1969)

β

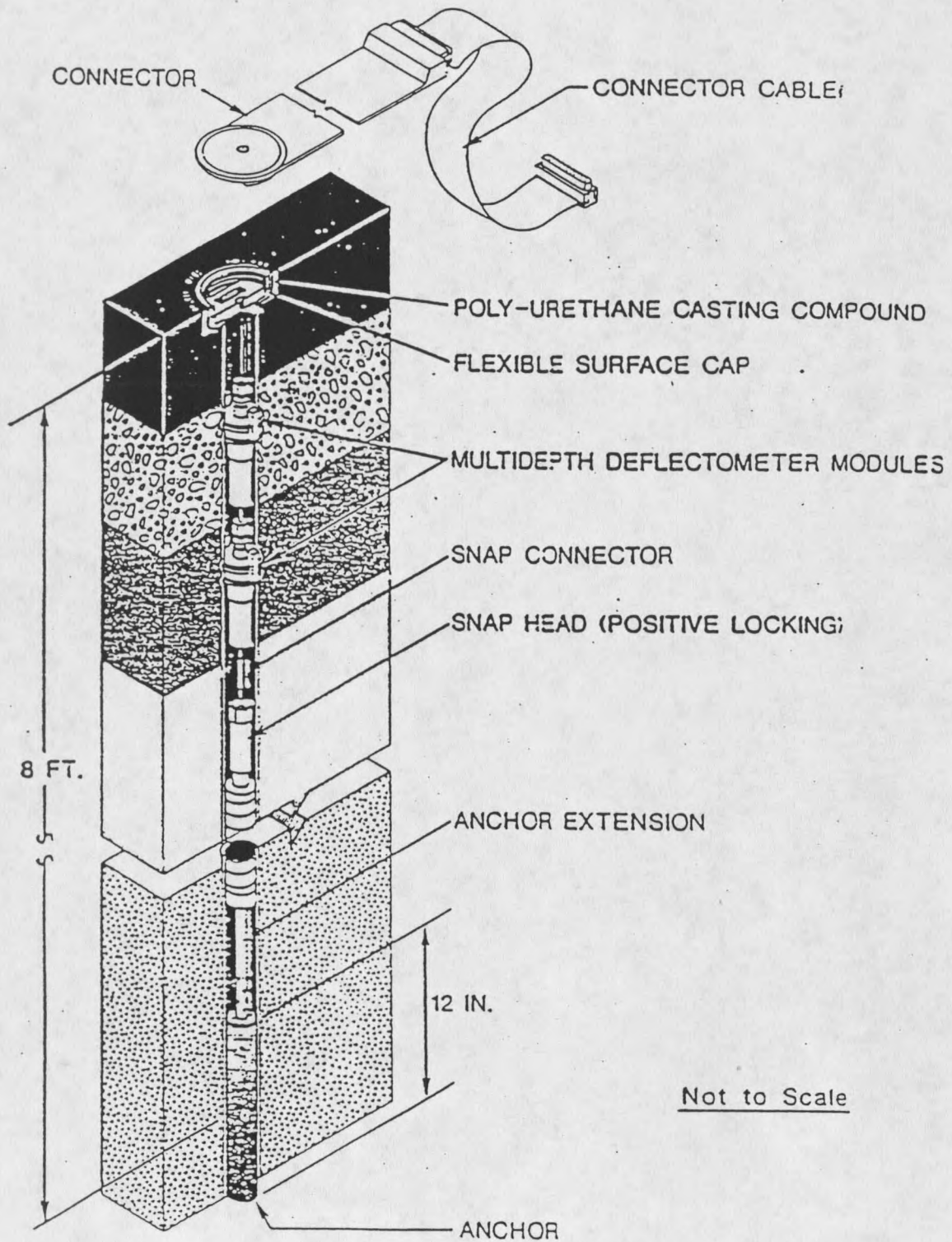


Figure 4. Cross section of a MDD after installation (from Pilson, 1995)

A MDD is installed by the following procedure. After drilling a core hole, a rubber wall liner is placed. Then an anchor is cemented into the bottom of the core hole. The lowest MDD module is then lowered into the core and tightened against the core wall at the desired depth. An inter-connecting rod is fastened from the module to the anchor at the base of the core. Successive modules are then lowered into the core hole, fixed against the wall and connected to the previous module. Ducting in each module allows for the wiring to run up the core hole. This technique allows measurements to be taken at any depth in the roadway. The MDD can measure either relative elastic deformations between points or total deformations from the anchor depth.

### Instrumented Roadways

#### Full Scale Tests

Mn/ROAD. Mn/Road is the largest and most extensive instrumented roadway in the world (WWW, 1996). Located 64 km northwest of Minneapolis, Minnesota on I-94, the facility has 8.8 km of roadway instrumented with over 4500 sensors. Opened in 1994, the project is expected to have a life time of 20 years. The primary objective of the facility is to provide findings which will help to develop better fundamental approaches to pavement design and maintenance (Newcomb, 1989). The facility incorporates a variety of testing options. A 4.8 km long high-volume traffic section exists on the west bound lane of I-94. The design average daily traffic for the roadway is 24,200 vehicles, 3200 of which are classified as heavy commercial vehicles. A weigh in motion (WIM) device is located at the

start of the high-volume traffic section to record the actual count of heavy vehicle traffic. The low-volume traffic roadway is a 4 km closed loop road north of the interstate. Loading for it consists of a known number of truck passes at the legal weight limit (355 kN) and above the legal limit (454 kN).

The Mn/Road facility uses AC and portland cement concrete over 6 types of aggregate bases. The roadway structure does not contain any geosynthetics. The existing subgrade in the area is a loam with an AASHTO classification of A-6 and an R value on the order of 15. In addition to the native subgrade, the low-volume road will import a heavy clay with an R value of 5 for 3 of its test sections. Ground water levels over the entire site vary from 7.62 cm above the grade to a depth of 4.26 m.

Strain instrumentation of Mn/Road is located in the cemented surfaces of the roadway. Six types of strain gauges are utilized. One type is the Alberta Research Council biaxial gauges, which consist of 4 foil strain gauges embedded in asphalt mastic mix. Two of the foil strain gauges are oriented in the longitudinal direction while the other two are rotated 90° to measure strain in the transverse direction. A total of forty of these gauges were installed. H-gauges consist of 230 Dynatest PAST-2AC/CC gauges. The most numerous gauge is the Tokyo Sokki PML-60 of which 436 were installed. This gauge is similar to an H-gauge with the removal of the two metal bars on each end. A coarse grit coats the surface of the gauge to help bond the gauge to the cemented material. Vertical displacements are measured by Schaevitz HCD-500 LVDT'S. One-hundred and sixty two Geokon VCE 4200 vibrating wire strain gauges are used in the rigid pavement sections. Their purpose is to measure warp in the slabs, which can be correlated to temperature, moisture, and shrinkage.

Center for Transportation Research, University of Texas, Austin. Conducted as a preliminary study, Pilson (1995) instrumented a flexible pavement roadway to investigate the best instruments and locations for follow on studies with the Texas Mobile Load Simulator. The roadway used was located in Victoria, Texas and consisted of thin and thick test sections. The thin section had a 5.08 cm AC surface over a 30 cm base course. The thick section was identical to the thin section, but used 19.8 cm of AC. Loading was provided by a dump truck. Statistical analysis was performed on the data to determine the precision of each gauge.

Five types of H-gauges and a durable foil strain gauge capable of being placed directly into the AC without the aid of a core or carrier block were tested. All measurements taken were dynamic. The study concluded that the foil strain gauge, a Hottinger Baldwin Measurements model DA3, gave the most precise and accurate measurements. The recommended sampling rate was at least 100 Hz.

North Carolina Instrumented Highway. This study consists of a 12 km instrumented section of State Route #421 near Silver City, North Carolina. Begun in 1988, the main objective of the research project is to develop mechanistic relationships between stress and strain levels imposed by traffic for a variety of typical flexible pavements (Stubstad, 1989). The roadway structure is AC over cement treated base course (CTBC) or aggregate base course (ABC). Geosynthetics are not included in the roadway. Strain instrumentation for the study consists of 72 Dynatest H-gauges placed at the bottom of the AC layer. Although stress measurements are taken in the base course, no strain measurements are taken there.

Alberta Instrumented Highway. The Alberta Transportation Department operated an instrumented roadway northwest of Edmonton from 1973 to 1976. The purpose of the test facility was to provide detailed measurements of pavement structural responses for evaluating the effects of axle loads and loading configurations of pavements (Christison, 1978). The two lane roadway was built on a subgrade of highly plastic (CH) clay. Asphalt concrete surfaces of 28 cm and 18 cm were used. Instrumentation consisted of foil strain gauges embedded in carrier blocks, surface deflection gauges, and diaphragm pressure cells.

The study centered on the effects of vehicle velocity, surface temperature, and service age on surface strains and deflections. Loadings from a variety of axle weights and configurations were compared to a standard 80 kN single axle dual wheel configuration. Results show that surface strains and deflections from the standard 80 kN axle increased with service life, surface temperature, and decreasing vehicle velocity. Load equivalency factors calculated are in close agreement from those based on the AASHO Road Test.

TRRL Instrumented Highway. Constructed in 1968, this was the first study in which vertical, longitudinal, and transverse measurements of stress and strain were taken in a full scale roadway (Potter, 1969). The study was conducted by the Transportation Road Research Laboratory (TRRL) on the A1 trunk road at Conington, Huntingdonshire (UK). The primary use of strain gauges was in the bottom of the AC surface layer. Eighty-nine early generation H-gauges were used of which 36 were damaged during construction. Twenty-two foil strain gauge imbedded carrier blocks were also used, of which only 5 survived construction. Additionally, 5 modified variable reluctance transducers, (similar to

an LVDT) measured strain in the base course. Dynamic measurements were made with loadings from a single unit truck every six months while normal commercial traffic provided the loading for long term measurements.

### Laboratory Tests

VPI, 1995. Conducted at the Virginia Polytechnic Institute, this study investigated the potential benefits of geogrid and geotextile reinforcement in flexible pavements, (Smith, 1995). Geosynthetic reinforced roadway structures were constructed in a reinforced concrete box of dimensions 3 m by 1.82 m by 2.13 m wide. A pneumatically driven circular loading plate applied a 40 kN force at a frequency of .5 Hz. Fifteen flexible pavement test sections were studied.

Each highway structure was composed of four materials. The subgrade consisted of 1.22 m of Yatesville Silty Sand (YSS) with an AASHTO classification of A-4. A geosynthetic was placed at the interface between the subgrade and the base course. Geosynthetics consisted of the Amoco 2002 and 2016 geotextiles, and Tensar SS2 geogrid. The aggregate used had a USCS classification of GW and a maximum dry density of 23 kN/m<sup>3</sup> at an optimum water content of 5.8 % measured by a Modified Proctor test. The hot-mix asphalt (HMA) wearing surface had a resilient modulus of  $1.72 \times 10^6$  kPa.

Measurements of the roadway consisted of surface deformations of the pavement. There was no internal strain instrumentation. The surface deformation was measured with an array of 8 LVDT'S attached to the support structure of the loading plate. Two of the LVDT'S were attached to the loading plate itself and the other 6 were placed at 15.2 cm

intervals. Loading took place until failure occurred, which was defined as 2.54 cm of permanent deformation in the section surface. Depending on the roadway structure, this could take over 6000 cycles.

The study found that two to three times the number of ESAL repetitions could be applied to geotextile reinforced pavement sections compared to unreinforced sections. Use of geogrid reinforcement did not alter the number of ESALs the roadway was capable of supporting. Researchers concluded that the separation function provided by geosynthetics is a key component for improving the performance of the pavement structure.

Danish Road Testing Machine. Designed and built in the 1970s, the Road Testing Machine (RTM) allows fatigue testing of pavement structures under controlled climatic conditions (Ullidtz, 1979). The facility is enclosed in a building 27.4 m in length, 4 m wide, and 3.8 m in height. The RTM itself consists of a pit 9 m long, 2.5 m wide, and 2 m deep. Hydraulic wheel loading consists of single or dual wheels. Maximum wheel load is 650 kN and maximum velocity is 25 kph. A schematic is provided in figure 5. The RTM is capable of applying 10,000 wheel loads in a 24 hour period. Because the RTM is enclosed, specific climatic conditions can be controlled. Temperatures range from  $-10^{\circ}$  C to  $+40^{\circ}$  C. Groundwater level in the pit is also controllable.

As of 1989, the RTM had been used in 5 major test programs. During this time the Danish RTM has witnessed the development of H-gauges. The gauges in the initial test program failed quickly. Upon excavation of the gauges extensive corrosion was determined as the cause of failure. Foil strain gauges mounted on cores were then tried. Initially these

gauges worked satisfactorily but eventually failed. Due to improvements in weatherproofing, survivability of H-gauges was not reported as an issue by Krarup (1992). Strains in the granular material are made using LVDT'S. Ullidtz (1979) performed finite element analysis to determine the effect of the LVDT'S on strain in the surrounding soil. It was found that results depended heavily on modeling assumptions of friction between the LVDT and the soil. With full friction, the LVDT would underestimate strain by 30%, while no friction would cause overestimation of 40%. Bison coils were also used, but were found not to be suitable for the dynamic measurements due to signal interference from the wheel loading apparatus.

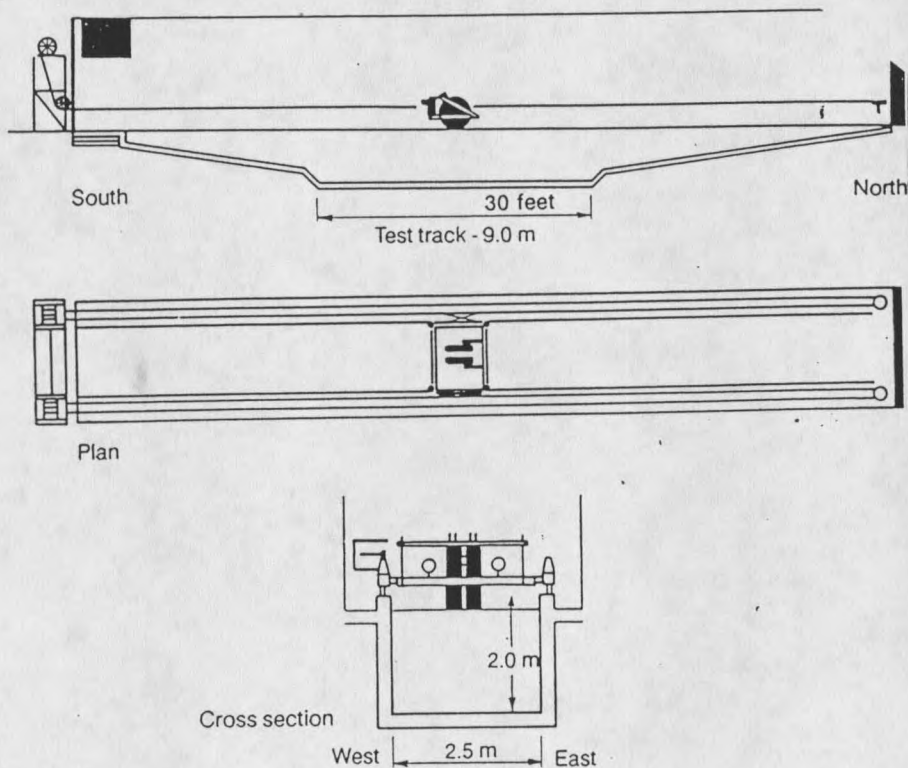


Figure 5. The Danish Road Testing Machine (from Krarup, 1992)

U.S. Army Engineer Waterways Experiment Station. Webster (1992) performed a study on the performance of geogrid reinforced base courses in flexible pavements for light aircraft. Sixteen different runway structures were built. Subgrade for the project was classified as a CH according to the Unified Soil Classification System. Base course material met FAA Item P-208 for Aggregate Base Course. The surface course of asphaltic concrete was not a test variable and was in all cases 10.2 cm thick. Six types of geogrid were used at varying depths in the roadway. Loading was provided by a 133 kN single-wheel-assembly cart. The cart was built on the frame of a cargo truck and used the wheel from a C-130 aircraft to apply the load.

Instrumentation consisted of four sets of MDD's. Modules were placed at 5 cm, 30.5 cm, and 61 cm below the surface, and the entire unit was anchored at a depth of 2.44 m. Although failure was defined as 2.54 cm of surface deformation, loading was usually continued up to 7.63 cm of deformation. Results showed that the amount of base course could be reduced through the use of geogrid reinforcement. Geogrid performance was determined to be a function of depth and for subgrade strengths greater than 1.5 CBR, the optimal reinforcement performance took place with the geogrid at the base course- subgrade interface.

University of Waterloo. Work performed at the University of Waterloo in 1985 studied the possibility of developing structural equivalency factors for geogrid reinforced base sections (Penner et al., 1985). The study was conducted by constructing numerous roadway structures in a laboratory and subjecting them to cyclic plate loading. The roadway

cross sections were built in a 4.5 by 1.8 by 0.9 m plywood box reinforced by a steel frame. An MTS function generator and servo-hydraulic controller were used to drive a 300 mm diameter loading plate onto the roadway surface. The loading force was 40 kN applied at a rate of 8 Hz followed by a single static load at predetermined cycle counts. Instrumentation consisted of dial gauges to measure the deformation of the AC surface and foil strain gauges bonded to the geogrid.

Various depths and types of materials went into the roadway resulting in 24 unique cross sections. The subgrade consisted of a very fine grained beach sand either pure or mixed with peat. The base was of quality well graded aggregate. The AC surface was a dense graded material with 15 mm maximum particle size mixed with 85/100 penetration grade asphalt cement. The geogrid used was biaxial polypropylene Tensar Corporation SS1.

The conclusion seemed to indicate that the geogrid reinforcement was significant in cases where inadequate base course thicknesses existed. The AASHTO design method was modified by the addition of granular layer coefficients. The coefficients measured the ratio of reinforced to unreinforced base layers and ranged from 1.4 to 1.8. Rutting in the subgrade decreased with the use of reinforcement.

### Tension Testing of Geosynthetics

#### Introduction

The goal of tension tests on geosynthetics is to measure material indices that are accepted throughout the industry. At this point, the difference between material indices and material properties should be made clear. Material indices are dependent on the testing

procedure used. An example for geosynthetics is the index of puncture resistance. A material property is intrinsic to the material, such as the modulus of elasticity. Because rate of strain and coupon size have been shown to change results in geosynthetic tension testing, results from these tests are classified as indicies.

To perform useful tension tests on geosynthetics, a test procedure must meet two criteria. The test must accurately resemble the state of the geosynthetic in use and be simple enough to enable comparative testing. If the test is complicated and difficult to reproduce it will not gain general acceptance. This section of the thesis reviews a widely accepted tensile test (ASTM Standard D 4595-86) and then considers the affect of test parameters on measured tensile properties of a geosynthetic.

#### ASTM Standards

Standard Test Method for Tensile Properties of Geotextiles by the Wide-Width Strip Method (D 4595-86) covers unconfined tensile properties of geotextiles. The test is characterized by a constant rate of extension (CRE) and 200 mm wide specimen. The specified strain rate is 10 %/min with a 3%/min tolerance. If the testing machine is not capable of running at a constant rate the standard will allow for an approximate strain rate of 2 %/min to be applied manually. In addition to being 200 mm wide, the specimen must be at least 100 mm long. The test is run until rupture of the specimen occurs.

Strain is obtained from jaw to jaw measurements. Strain gauges may be placed in the specimen center and through comparison with the jaw to jaw measurements slippage in the clamping system identified. The two clamp designs permitted are shown in figures 6 and

7. Both types of clamps operate on the principle of constricting the geosynthetic between a wedge and a fixed surface. As tension is applied by the testing machine, the geotextile pulls the wedge into a continually constricting space, thereby providing a tighter grip.

### Laboratory Testing

Three testing parameters have been found to significantly affect the measured tensile properties of geosynthetics. They are the grip system, specimen dimensions, and rate of strain. Gripping systems have been broken down into 3 main techniques. The mechanical wedge (used by ASTM) uses increasing friction of a wedge being pulled into a confined slot to hold the geosynthetic. This is the best technique and allows the least amount of slip. It is also typically more expensive to manufacture and difficult to mount the specimen in. As a consequence, materials testers have looked to other gripping techniques (as this study did). An alternative gripping technique is the roller grip or capstan. With this technique the geosynthetic is wrapped several times around a cylinder. As tension is applied, the outside layers of geosynthetic press against the interior rolls holding the geosynthetic in place. Although simpler, significant slippage occurs with this technique as higher tensile loads are applied. The third technique is to encapsulate the specimen to the grips using epoxy. This technique is good for low strength geosynthetics, particularly geotextiles which have large surface areas as compared to geogrids.

The varieties of geosynthetics and gripping techniques makes selecting a universal solution difficult. Myles (1986) found that there is no single gripping method suitable for all geotextiles. High strength geotextiles are difficult to grip in mechanical compressive jaws

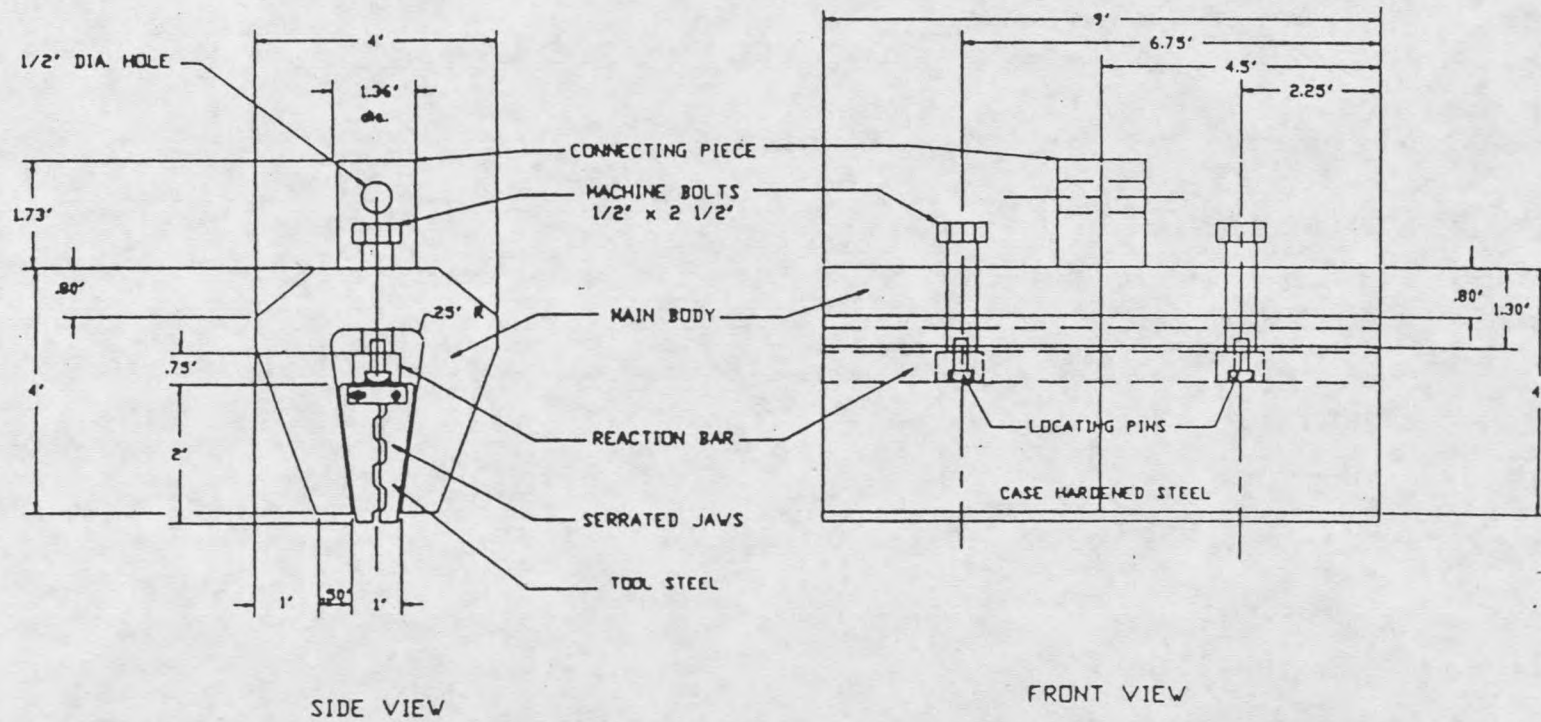


Figure 6. ASTM approved Sanders Clamp (from ASTM, 1993)

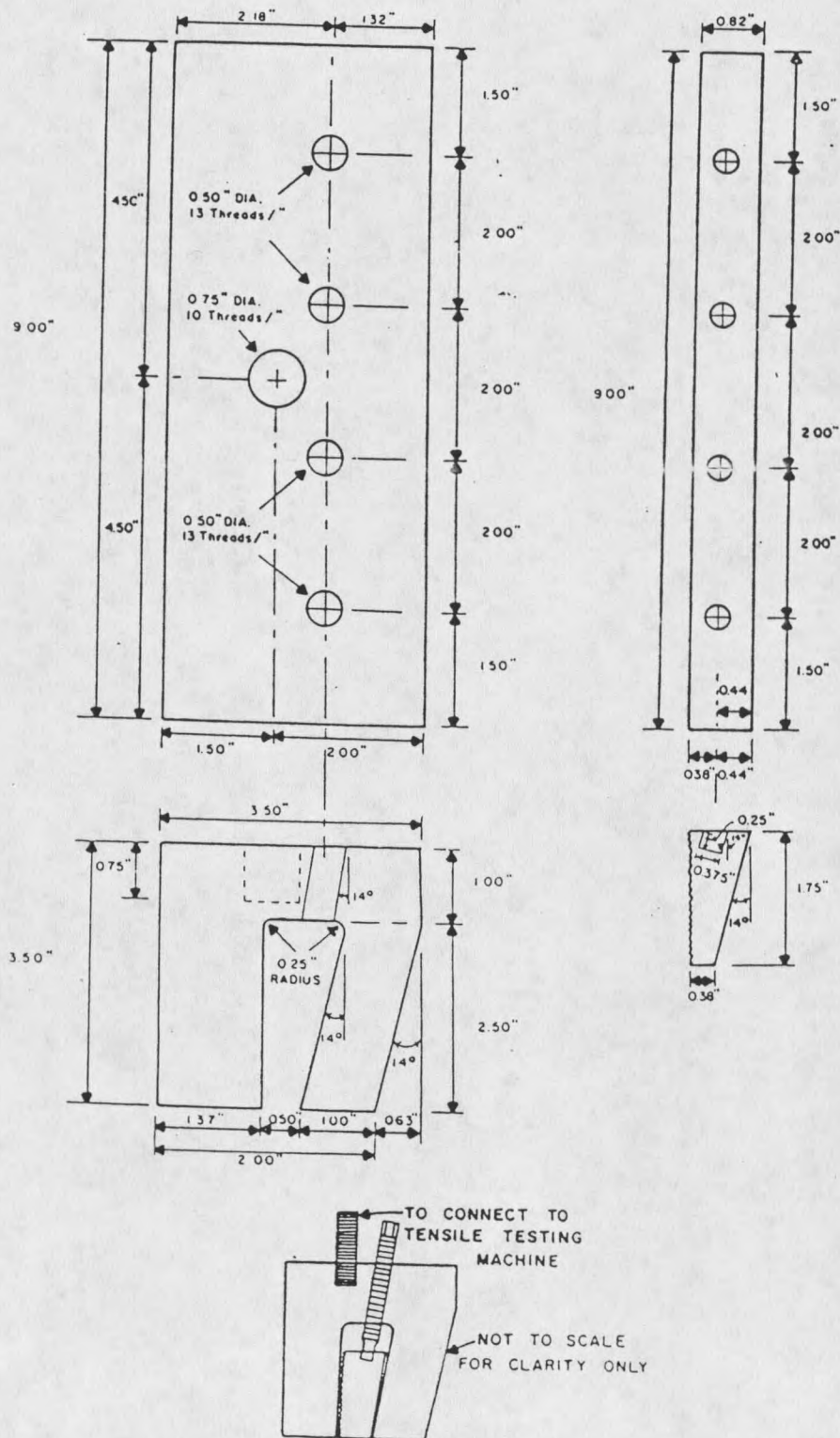


Figure 7. ASTM approved Wide Width Clamp (from ASTM, 1993)

and low strength, highly extendible non-woven geotextiles are often difficult to use in capstan type jaws.

Specimen dimensions have been shown to affect the measured strength of a material. The aspect ratio of the specimen is the ratio of width to length. Rowe studied a variety of geosyntheics and specimen dimensions. His results show that the modulus is dependant on aspect ratio and recommends specimens with gauge lengths of at least 100 mm and aspect ratios of 5 or greater be used. De Groot (1990) and Leshchinsky (1990) found similar results but do not recommend specific specimen dimensions.

It has been suggested that the rate of strain in geosynthetic tension testing is too high and new rates need be applied. Myles (1987) feels the rates of strain in existing "textile" tension tests are too high for geotextiles and a lower rate would be more realistic. Rowe (1986) showed the ASTM rate of 10 %/min to be too high and suggests a rate of 2 %/min. The lower loading rates are recommended to more accurately replicate loading in actual geotechnical structures.

#### Related Instrumented Geosynthetic Studies

A significant number of studies involving instrumented geosynthetic reinforced retaining walls and embankments have been made. Electrical resistance strain gauges have been used almost exclusively to measure strains developed in the geosynthetics of these projects. In order to make accurate and reliable measurements, the inherently difficult task of bonding a foil gauge to the geosynthetic must be accomplished. Review of existing literature indicates that there have been many different techniques used to bond foil strain

gauges to geosynthetics. This section is a review of those techniques.

Bathurst (1990) has performed studies on large scale geosynthetic reinforced soil walls. After much experimentation, he developed a mounting technique for applying Showa Measuring Instruments gauge type Y11-FA-5-120 to polypropylene geogrids. The geogrid surface preparation includes abrading with light sand paper, cleaning, and application of a neutralizing agent. The bonding agent used is a RTC two-part epoxy resin cement. Environmental protection is provided by a bubble of silicon and outer wrapping of flexible plastic tubing. This procedure allowed strain measurements of up to 3% and survival rates of 100% to be common during his testing routine.

Prior to his study of a geogrid reinforced test wall, Simac (1990) also conducted an extensive laboratory calibration program to identify high elongation foil resistance strain gauges that were compatible with the stress/strain characteristics of the geogrid in his study. A Kyowa Dengyo gauge type KFE-5-C1 bonded with high elongation cyanoacrylate adhesive type CN from Tokyo Sokki Kenkyujo Company was ultimately selected. Weatherproofing was provided by application of an elastic asphaltic emulsion. The study reported strain levels up to 2 % but does not discuss failure rates.

Rowe (1994) measured geotextile strain in a full scale embankment in order to monitor the structure's performance through construction and deliberate overloading to induce failure. The study used Micro-measurements gauge type EP-08-40CBY-120 protected by Dow Corning 3145 RTV adhesive/sealant to monitor strains in a geotextile. Of the 38 gauges planned for this study 5 did not survive installation and 4 others failed during the course of the study. This mounting technique was adequate to strain levels of about 5%.

Leshchinsky (1990) conducted studies to determine techniques for using foil strain gauges in laboratory tension tests of geotextiles. He used elastic silicon from Teroson GmbH called Terostat 33 Silicone Sealant to mount Micro-Measurements EP-08-40CBY-120 gauges to geotextiles. Although strain rates of up to 10% were possible with this method it is not clear whether the procedure could be weatherproofed for use in a working environment.

Oglesby (1992) studied techniques for using foil strain gauges to measure high strains (over 5 %) during unconfined tension tests of geogrids. This was a preliminary study to develop methods for confined tests and eventually full scale field applications. Variables included surface preparation techniques, adhesives, clamping techniques, and strain gauges. For high density polyethylene, the recommended procedure is to prepare the surface with steel wool and sand paper. After cleansing with alcohol, Micro-Measurements EP-08-250BG-120 gauges are bonded with A-12 adhesive. Uniform pressure on the gauges is provided by clamping the area between neoprene pads. The geogrid is then oven cured at 125° Fahrenheit for at least 4 hours.

## CHAPTER 3

## RESEARCH METHODOLOGY

Introduction

The purpose of this chapter is to present the experimental methods and equipment used in the study. The chapter is divided into sections on the instrumented roadway and the wide width testing facility. The instrumented roadway section contains descriptions of strain sensors, data logging systems, roadway monitoring, roadway construction, and emplacement of sensors. The second section describes the wide width tension testing facility and experiments performed with the apparatus.

Instrumented RoadwayInstrument Types

Four different types of sensors were evaluated in the study. They were selected such that dynamic and static measurements could be taken. Three sensor types were placed in the base course and on the geosynthetics, while only one type was used in the asphalt concrete. All the sensors were placed in a horizontal plane oriented to measure strain perpendicular to the direction of traffic (the transverse direction in the case of the geosynthetics).

Asphalt Concrete. Geokon (Lebanon, NH) model VCE-4200-HT (high temperature) vibrating wire embedment strain gauges were used in the asphalt concrete. The gauge is shown in figure 8. Vibrating wire technology was selected because it is excellent for long

term measurements. They measure strain by determining the frequency of a vibrating wire that runs in the shaft of the gauge. A mechanical device plucks the wire and the resonant frequency is measured. Knowledge of the frequency allows calculation of the length of the wire and hence the length of the gauge. Knowing this information allows the strain to be easily calculated. Vibrating wire strain gauges can be used with long cable lengths because their output signal is a frequency which is not susceptible to degradation caused by changes in cable resistance. This is an advantage compared to foil strain gauges, which use voltage for signals and are susceptible to changes in cable resistance. The major disadvantage of vibrating wire technology is their slow response. Several seconds are required to pluck the wire and obtain the resonant frequency. This makes dynamic measurements impractical with the gauges.

The active gauge length of the gauge is 150 mm. Range of the gauge is 0.3 % strain (3000 micro strain) with a sensitivity of 0.0001 % strain (1 micro strain). High temperature resistant Teflon cable is used with the gauges to withstand placement in the asphalt concrete. A thermister is also included in the gauge. Four of the gauges were used in the roadway.

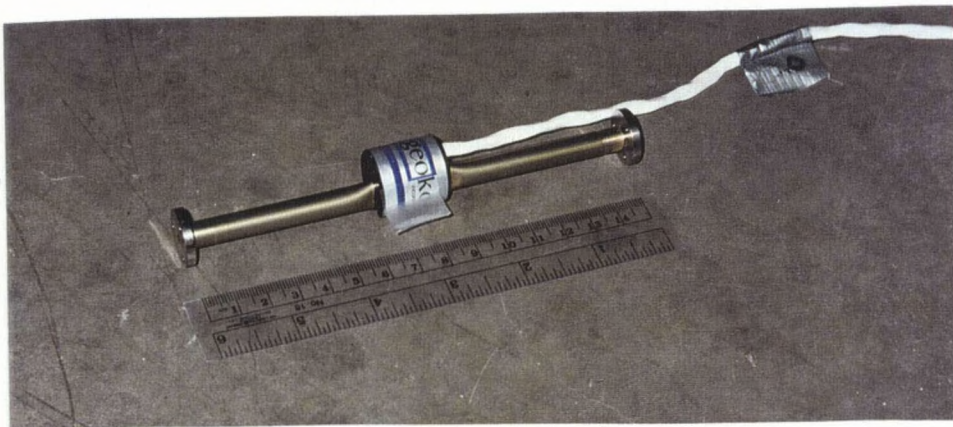


Figure 8. Vibrating Wire Embedment AC Strain Gauge

Instrumentation in the Base Course. Geokon model VCE-4200 vibrating wire embedment type strain gauges (shown in figure 9) were one of three gauge types used in the base course. The instrument is identical to the HT model used in the AC with two exceptions. High temperature Teflon cable is not used and the end discs are larger (76 mm in diameter) to produce better interaction between the base material and the sensor. A thermister is also included in the gauge. Two of the gauges were used in the roadway.

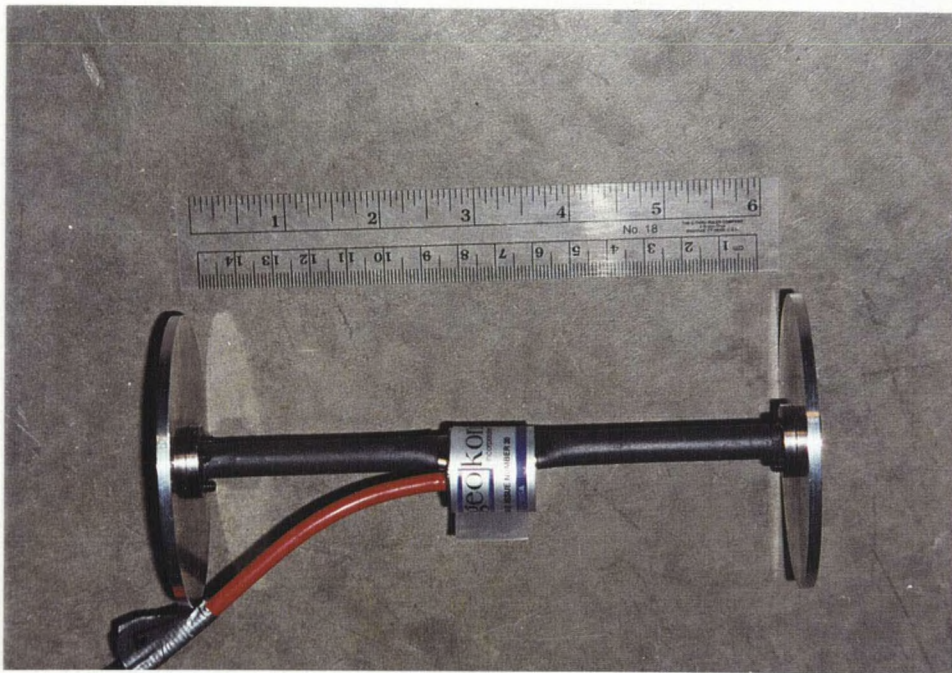


Figure 9. Vibrating Wire Embedment Strain Gauge

For measuring larger displacements in the base course, vibrating wire embedment displacement gauges were used. Originally, two Geokon model 4430 vibrating wire borehole deformation meters were to be used. During installation however, one of the sensors was found to be defective and in its place a model 4420 vibrating wire crack meter was used. The two sensors have the same physical dimensions and operate in the same manner.

The vibrating wire displacement gauges operate on the same principle as the vibrating wire strain gauges. The major difference between the two sensors is the range of displacement measured. The embedment displacement gauges have a range of 8 % while the strain gauges had a range of only 0.3 %. A vibrating wire displacement gauge is shown in figure 10. The end discs are 101 mm in diameter and the length of the instrument is 317 mm. The sensitivity of the gauge is 0.008 %. Thermistors are included in each gauge. One each of the model 4430 and 4420 were used.



Figure 10. Vibrating Wire Embedment Displacement Gauge

To measure both the static and dynamic performance of the base course, embedment LVDTs were utilized. Shown in figure 11, the models chosen were RDP Electronics (Pottstown, PA), submersible, miniature AC, model D5/400W LVDTs with a range of +/-

10.2 mm and a sensitivity of  $\pm 0.03$  mm. For the gauge length of the instruments, this corresponds to strain measurements of  $\pm 13\%$  and a sensitivity of  $\pm 0.04\%$ . The end discs of the LVDT's have diameters of 39 mm and the length of the sensor is 81 mm. Four of these instruments were used in the roadway.

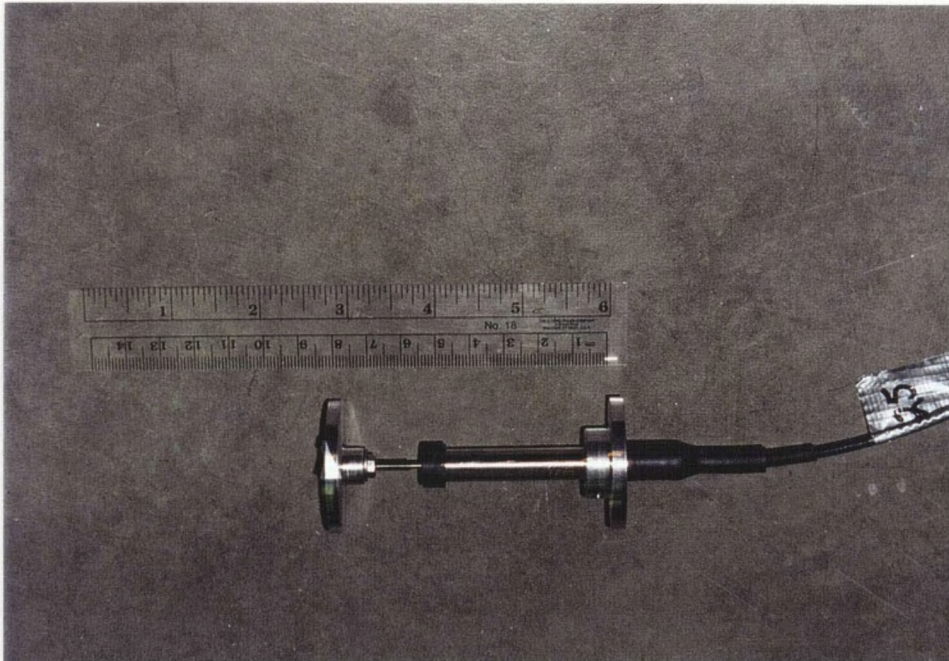


Figure 11. LVDT Embedment Strain Gauge

Instrumentation on the Geosynthetics. Vibrating wire, LVDTs, and foil strain gauges were used on the geosynthetics. Figure 12 shows a vibrating wire strain gauge used for long term measurements. The sensor was attached by sandwiching the geosynthetic between two rectangular mounting plates measuring 89 by 57 mm. The plates were held together with 6 bolts. The strain gauge itself was mounted to the steel plate by means of a circular collar and held in place with a set screw. When mounted, the axis of the strain gauge was

approximately 14 mm above the surface of the geosynthetic. Two of these gauges were used in the roadway.

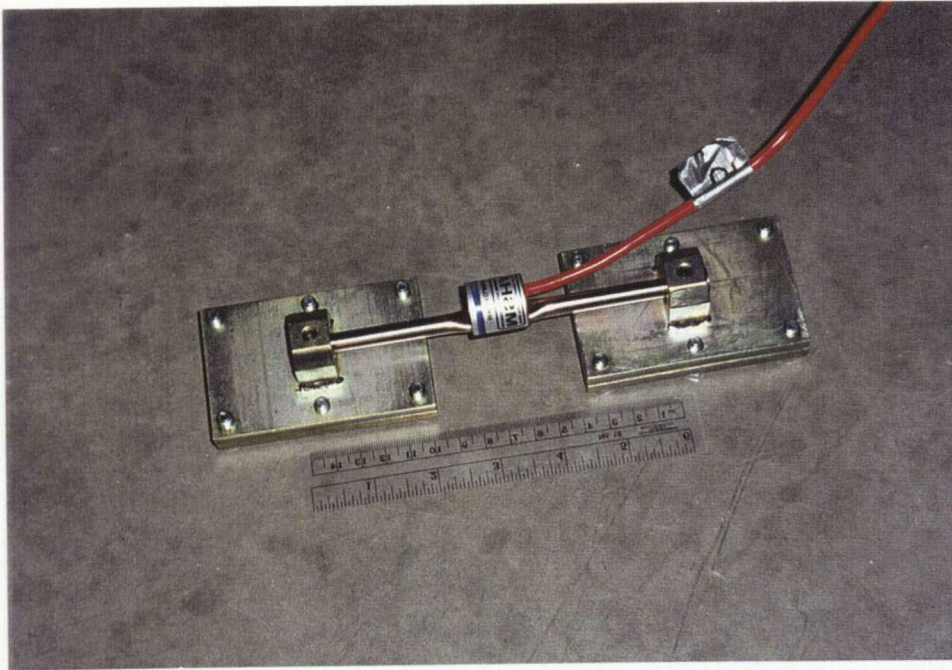


Figure 12. Vibrating Wire Strain Gauge

To measure large static strains in the geosynthetics, vibrating wire displacement gauges were used. The model selected was a Geokon model 4420 vibrating wire crackmeter shown in figure 13. The gauge has a range of 25.4 mm and a sensitivity of 0.025 mm. The nominal gauge length of the instrument is 280 mm, which allows a strain range of 9 % with a sensitivity of 0.009 %.

The method used to mount the vibrating wire displacement gauge to the geosynthetic was similar to that used for the vibrating wire strain gauge. Each end of the gauge was connected to a rectangular mounting plate measuring 89 by 57 mm. The geosynthetic was

sandwiched between the plate and an identical mounting plate. Six bolts were used to hold the plates together. A ball pivot point connection was utilized between the gauge and the plates which allowed any orientation of the mounting plate. The axis of the gauge was approximately 25.4 mm above the surface of the geosynthetic. Two of the gauges were used in the roadway.

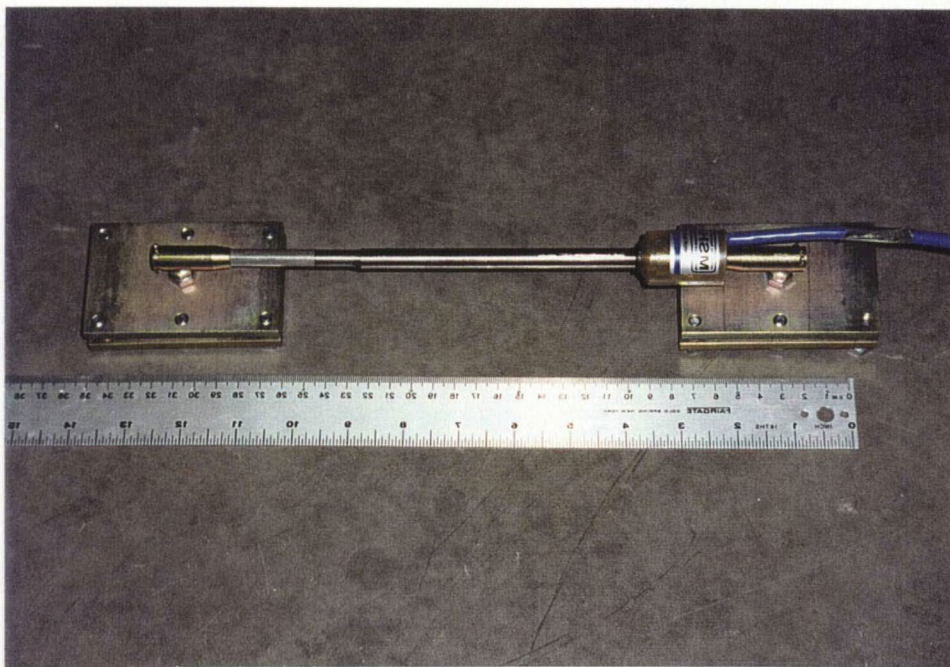


Figure 13. Vibrating Wire Displacement Gauge

The LVDT used on the geosynthetic was an RDP Electronics submersible, miniature AC model D5/200W LVDT with a range of  $\pm 5.1$  mm and a sensitivity of  $\pm 0.015$  mm. Shown in figure 14, the gauge measured both dynamic and static strains. Given the 50 mm nominal gauge length of the instrument, this device has a strain range of  $\pm 10\%$  and a sensitivity of  $\pm 0.03\%$ .

The mounting brackets for the LVDT were small compared to those used by the VW technology. They measured 30 by 12 mm and were fixed in orientation. The axis of the gauge was approximately 14 mm above the surface of the geosynthetic. Four of the gauges were used in the roadway.

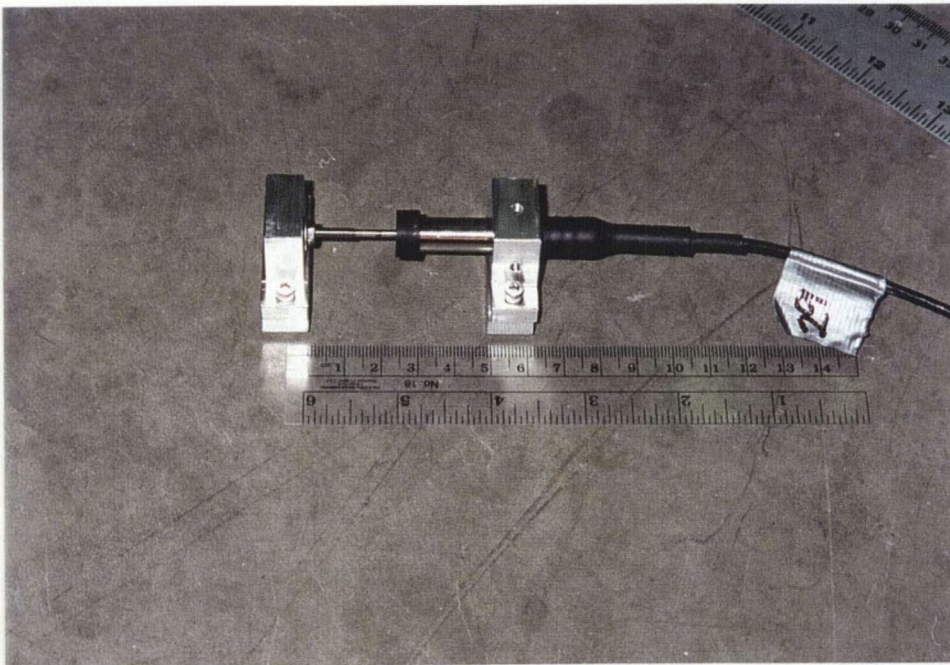


Figure 14. LVDT Displacement Gauge

Kyowa (Soltec Corp., San Fernando, CA) high elongation foil strain gauges (model KFE-5-120-C1) were used directly on the geogrid. Due to their small size (approximately 3.4 by 11 mm) they could be mounted on an individual rib of the geogrid. Foil strain gauges were not used on the geotextile. The foil strain gauges have excellent response for dynamic measurements, but are unsuitable for long term measurements due to drift in their signal as discussed previously.

The following procedure was used to bond the foil strain gauges to the geogrid. The surface was prepared by sanding with 600 grit sand paper. The rib was then etched with MicroMeasurements Tetra-Etch (TEC-1). Next, the surface was rinsed with water and allowed to dry. A single gauge was attached to the upper side of the geogrid using MicroMeasurements M-Bond AE-10. An additional gauge was attached to a small, detached sample of the geogrid. The two gauges were attached by a full wheatstone bridge circuit and connected to 2-pair, twisted pairs, overall shielded, 22 gauge cable. The gauge attached to the unstressed sample of geogrid provided for temperature compensation. This bonding procedure appeared to be adequate for the small strains that were ultimately observed in the field. Additional laboratory tension testing, however, indicated that gauge debonding occurred at 1-3 % strain.

Environmental protection of the gauges was provided by sandwiching the geogrid area between sheets of MicroMeasurements M-Coat F Butyl rubber sealant and neoprene. Additional protection was provided by sandwiching this area between sheets of clear plastic with liberal amounts of silicone use between the sheets, particularly around the cable entry. Finally, the entire area was sandwiched between sheets of geotextile, again with liberal amounts of silicon applied. Four of the foil gauges were used in the roadway.

#### Data logging Systems

Two data logging systems were used in the study. One was designed to handle the long term recordings and the other dynamic recordings.

Long Term Data Logger. The long term data logger was a Campbell Scientific (Logan, UT) data logger, Model CR-10. Supporting equipment included 2 AM-416 16 channel multiplexers (all 16 channels of a multiplexer were routed into one channel of the logger), one AVW1 Vibrating Wire Interface (provides excitation for all VW gauges), PS12LA Power Supply (12VDC and battery), SC32A RS-232 Interface (allows communication directly through a PC serial port), and a DC112 Modem (1200 baud modem for remote access to the data). The CR-10 system is designed for stand-alone field data acquisition and storage at relatively slow rates. It can interface to all types of sensors including VW gauges, sensors with DC outputs, and all types of temperature sensors.

The Campbell data logger was programmed to record data every hour, 24 hours a day. The data recorded for each hour was data averaged over a 10 minute period prior to the time of recording. The logger is capable of cycling through the 24 channels every 30 seconds, meaning that for the 10 minute data collection period, 20 samples per instrument were taken and averaged. The data was stored in the data logger and could be downloaded from a remote computer using the telephone modem or collected on site as needed.

Dynamic Data Logger. An IOTech (Cleveland, OH) Daqbook 100 was used as the dynamic data logger. A disadvantage of the unit was that it could not monitor the vibrating wire instruments. It could however, be readily adjusted to monitor only specific instruments or desired sampling rates. The logger included a DBK-40 BNC Analog Interface (16 channel box that allows BNC connections to be made). The Daqbook is basically an A/D converter that can communicate with a PC. It allows data to be collected and stored at various speeds.

Supporting electronic equipment was used by LVDT's and foil strain gauges. Signal conditioning for LVDT's was provided through a RDP Electrosense S7-AC signal conditioner, which provides an AC excitation and a +/- 10V DC output. This output could be read by both the Campbell logger and Daqbook. The foil strain gauges used a RDP Electrosense S7-DC signal conditioner with an excitation voltage of 5 V DC and the gain set to 260.

### Roadway Monitoring

Long Term Monitoring Program. The data logging began with the Campbell data logger on July 22, 1995 at 2:00 P.M. At this point in time the roadway was still under construction. The base course had been placed and spread but not compacted. The only transducers recording meaningful data were those attached to the geosynthetics. The first compaction of the base course took place on July 24th at approximately 7:00 A.M. The Campbell logger was turned off at this point such that the transducers could be monitored real time with the dynamic data logger to ensure that damage was not occurring during compaction. The next day, July 25th, the aggregate base course was compacted around the embedment transducers.

Following successful compaction of the base course, a series of tests were conducted on the unsurfaced roadway. On July 25th, four truck pass tests were conducted. At completion of the tests the Campbell data logger was turned back on. On July 31st, road rater tests and two more truck pass tests were performed on the unsurfaced roadway. At this point, the only transducers not providing meaningful data were the embedment strain gauges

for the asphalt concrete.

On August 1st the asphalt concrete running surface was placed. At approximately 7:00 A.M. the base course layer was leveled and compacted for a second time. The asphalt concrete was placed shortly thereafter with the embedment gauges placed in the AC. The asphalt was allowed to cure for several hours with the section being opened to truck traffic at 1:00 P.M. It is noted that the unsurfaced section was closed to traffic up until the time that the asphalt was placed.

The Campbell data logger was inoperable between August 3, 12:00 P.M. to September 7, 12:00 P.M. Any stored data was lost during this period. During the period, the logger was returned to the manufacturer for service. The malfunction was due to a bad diode which was replaced. During this time, dynamic data could still be collected. A truck pass test was performed on August 29. Additional Road rater tests were performed on the surfaced roadway on September 21st. The final two truck pass tests were performed on the AC surfaced roadway on October 19.

The logger was permanently disconnected on October 26. The roadway itself, was dismantled in early November and all instrumentes, with the exception of the AC vibrating wire embedment strain gauges were retrieved. A history of the significant events concerning the roadway is shown in Table 1. The truck pass tests and road rater tests are discussed in the next section.

Dynamic Monitoring Program. The dynamic testing program recorded the response of the instruments to individual loadings on the roadway. Truck pass tests were conducted by a variety of different sized trucks operating in the yard. Road Rater tests were conducted

Table 1. Chronological Order of Events For Roadway Construction and Testing

Date	Time	Event	Reference Times (hours)
July 22	2:00 P.M.	Campbell data logger turned on, uncompacted base in place.	--
July 24	7:00 A.M.	Base course compacted.	0
July 25	7 A.M. - 2 P.M.	Base course transducers set, truck pass tests 1-4.	22-29
July 25	3:00 P.M.	Logger turned back on.	31
July 31	10:00 A.M.	Road rater and truck pass tests 5 & 6 on unsurfaced section.	170
Aug. 1	7:00 A.M.	Base leveled & recompacted, AC placed and compacted.	191
Aug. 1	1:00 P.M.	Section open to traffic.	197
Aug. 3-	12:00 P.M.	Campbell data logger	242-1083
Sept. 6	12:00 P.M.	inoperable	
Aug, 29	8:00 A.M.	Truck pass test 7	864
Sept. 21	9:00 A.M.	Road rater tests	1441
Oct. 19	8:00 A.M.	Truck pass tests 8 and 9	2112
Oct. 26	5:00 P.M.	Logger disconnected	2289

by the Non-Destructive Testing Unit of the Montana Department of Transportation (MDT). The Daqbook, described earlier in this report, was used to collect data from the non-vibrating wire instruments during these tests. During the second Road Rater test performed on September 21st, monitoring programs were downloaded to the Campbell logger to enable it

to cycle through one channel at a time, such that the Road Rater could be placed in the vicinity of a vibrating wire instrument with data from this instrument being taken at a rate of approximately 1 sample every second.

For the truck pass tests, the non-vibrating wire instruments were monitored as trucks were allowed to slowly pass over the test section. The trucks typically traveled at a speed of 8 kph. Tests were performed prior to and after the placement of the AC layer. Four types of trucks were used for the nine truck pass tests listed in Table 1. Truck pass tests 1 and 2 used a 2-axle pickup truck weighing approximately 15 kN. An empty belly dump truck weighing 156 kN was used for truck pass 3. A single unit dump truck with a pup trailer was used for truck pass 4. Both the truck and pup were full with gravel. A weight of each unit was not obtained. A full single unit dump truck with a pup trailer was used for truck pass tests 5 and 6. The entire vehicle weighed 423 and 406 kN for tests 5 and 6, respectively. Tests 1-6 were performed on the unsurfaced test section. The record of the truck used for test 7 was not available. A full belly dump truck weighing 414 and 429 kN was used for truck pass tests 8 and 9, respectively. Tests 7-9 were performed on the surfaced test section. A summary of the truck data for the different tests is given in Table 2.

Road Rater tests were performed for the purpose of evaluating the ability of the instruments to respond to the dynamic surface load. The tests were also conducted for the purpose of determining whether this was a suitable means of providing dynamic response data for use in follow on research. Although not a primary objective, the Road Rater tests were also used to back calculate elastic moduli for the various pavement layers.

Table 2. Vehicles Used For Truck Pass Tests

Test #	Date	Truck Type	Weight, kN	Surfacing
1	July 25	Pickup	15	Unsurfaced
2	July 25	Pickup	15	Unsurfaced
3	July 25	Belly Dump (empty)	156	Unsurfaced
4	July 25	Single Unit With Pup	not known	Unsurfaced
5	July 31	Single Unit With Pup	423	Unsurfaced
6	July 31	Single Unit With Pup	406	Unsurfaced
7	Aug. 29	Unknown	not known	Surfaced
8	Oct. 19	Belly Dump	414	Surfaced
9	Oct. 19	Belly Dump	429	Surfaced

The first Road Rater tests on July 31st were performed on the unsurfaced test section after the base course was initially placed, compacted, and after base material was compacted around the embedment transducers. A model 2000 Road Rater (Foundation Mechanics, Inc., El Segundo, CA) machine was used for these tests and consisted of a circular plate 30.5 cm in diameter through which a dynamic load was applied over a period of time at a given frequency. Dynamic displacement transducers monitored the vertical deformation of the ground surface at points extending radially from the applied load. Dynamic displacement was measured at points 0, 20.3, 30.5, 61, 91, and 122 cm from the center of the applied load. The load frequency was 25 Hz with the instrument sampling frequency set at 20 Hz. For the tests performed on July 31st, five multi-level force values were applied within a give load cycle, with this load cycle repeated 5 times for the majority of the test locations. The dynamic force levels were 6.67, 8.9, 11.1, and 13.3 kN. Each load in the load cycle was

applied for approximately 3-5 seconds, with the next load in the cycle applied immediately thereafter. For each test, the Road Rater loading plates were set on the ground surface directly above the instruments to be monitored.

The second series of Road Rater tests performed on September 21st were similar to the first series. The loading sequence consisted of four cycles of incrementing loads, where the loads were set at 11.1, 13.3, 15.6, and 17.8 kN. The frequency of loading was reduced from 25 Hz to 20 Hz with the instrument sampling rate increased from 20 Hz to 60 Hz in an attempt to capture the response for a given load application.

For the September 21st Road Rater tests, the Road Rater was also used to apply load atop the vibrating wire instruments. This was done to assess the possibility of using these instruments for dynamic measurements, provided the sampling rate could be sufficiently high. Individual programs were downloaded to the Campbell logger allowing for one vibrating wire instrument to be sampled and monitored. This approach increased the sampling time to approximately 1 Hz. The road rater was configured to apply four cycles of the same load, 17.8 kN, such that a near constant dynamic load could be applied to the instrument. The loading frequency was increased to 50 Hz in an attempt to make this load appear even more constant. Six of the twelve vibrating wire instruments were successfully tested. The 17.8 kN load was applied for approximately 100 seconds to each instrument.

### Roadway Construction and Gauge Locations

Introduction. The roadway was constructed in a local contractor's gravel quarry located between Bozeman and Belgrade. The contractor, JTL Inc., allowed for the

construction of the roadway along a truck travel path leading from the gravel pit to the weigh scale. The travel path was covered by a layer of deteriorating asphalt. JTL Inc. donated the raw materials (gravel base and asphalt concrete) and the equipment and labor necessary to construct the roadway. Construction of the roadway began on 13 July and was completed on 1 August, 1995.

The purpose of the roadway was to evaluate instruments that were thought to be suitable for use in the follow on research and whose likelihood for success was uncertain. The roadway was not chosen with the aim of duplicating the types of subgrade and layer thickness and preparation conditions anticipated in follow on research. While this would have been a desirable feature to incorporate in the roadway, cost and time limitations did not allow for such action.

Roadway Construction Overview. The roadway was constructed by excavating the existing asphalt and subgrade along a straight section measuring 42 m in length by 4.5 m in width. The existing asphalt was less than 5 cm thick. The existing subgrade consisted of a dry to moist, silty, sandy gravel with cobbles. The subgrade appeared to be at a relative density of 75-85 %. The excavation extended to approximately 26 cm below the top of the existing asphalt grade. Approximately 10 cm of the subgrade was scarified and recompactd with a vibratory steel drum roller. A thin layer of base course material was placed and spread to level the bottom of the excavation. This layer was not compacted and ranged in thickness from 1.27 cm to 5 cm. When completed, trucks entered the pit along the existing travel way to the west of the test section and returned by entering onto the test section when coming out

of the pit and traveling towards the weigh scale. In this way, the test section saw only loaded trucks whose weights were recorded at the scales.

A 16.7 m section of geogrid (Tensar BX 1100) was placed within the extreme Northeast end of the test section. A 13.7 m section of geotextile (Amoco 2006) was placed immediately to the Southwest of the geogrid section. The remaining 12.2 m of the test section to the Southwest was left as an unreinforced control section. A plan view of the test section is shown in figure 15.

The instrumentation for the geosynthetics was then attached. Instrument installation is detailed later in the thesis. Approximately 20.3 cm of base course was then placed and spread throughout the test section. It was a gravel with sand and silt, with no particle larger than 7.6 cm. Instruments were installed in the base as it was placed. The base course was placed with a large front-end loader and spread with a small skid-steer loader. It had to be hand-spread in locations where instruments were to be embedded. Then the base course was compacted with a vibratory steel-drum roller. Additional base course was placed and spread level with a grader and recompact with the same roller. Approximately 6.35 cm of asphalt concrete was then placed with a belly-dump truck, spread level with a grader and then compacted with a steel-drum vibratory roller.

Instrumentation Layout. A total of 24 instruments were placed in the roadway. The locations are shown in figure 16. The dashed lines running the length of the roadway show where the anticipated truck wheel paths were to be located. The embedment strain gages in the base and asphalt concrete were placed as close as possible to the bottom of the respective layers. A summary of the gauges used in the roadway is given in Table 3.

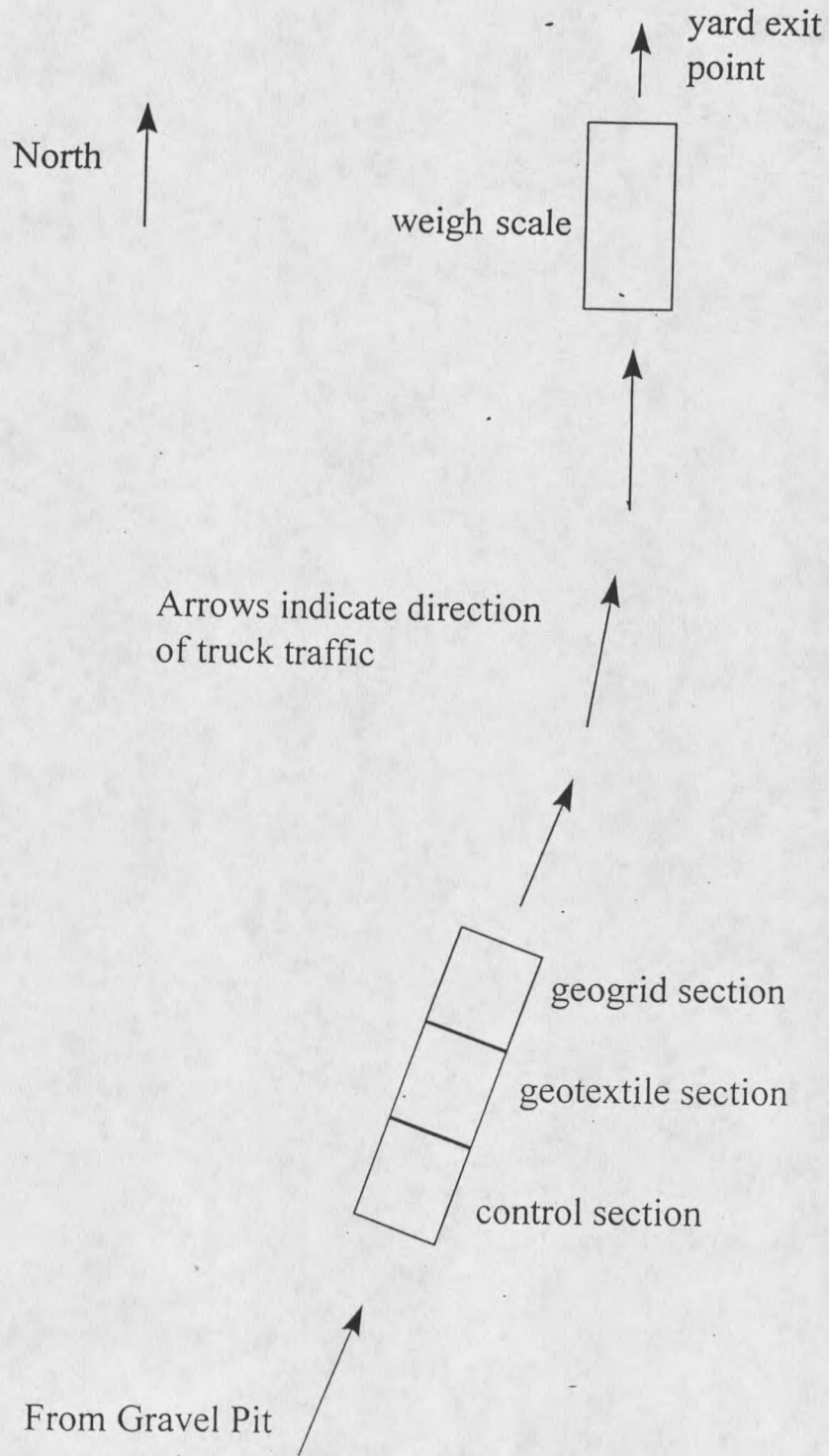


Figure 15. Plan view of Roadway Test Site

- VW Embedment Strain Gage in Base
- VW Embedment Displacement Gage in Base
- LVDT Embedment Gage in Base
- ⊗ VW Embedment Strain Gage in AC
- VW Strain Gage on Geosynthetic
- × VW Displacement Gage on Geosynthetic
- ⊗ LVDT on Geosynthetic
- △ Foil Strain Gage on Geogrid

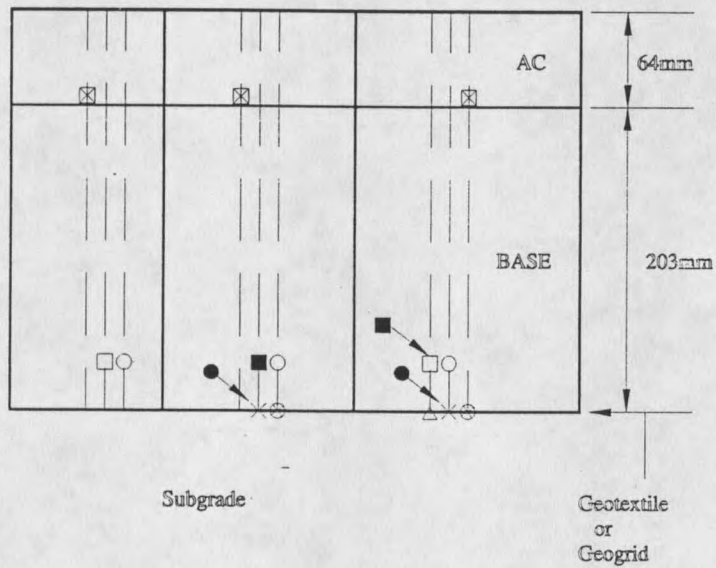
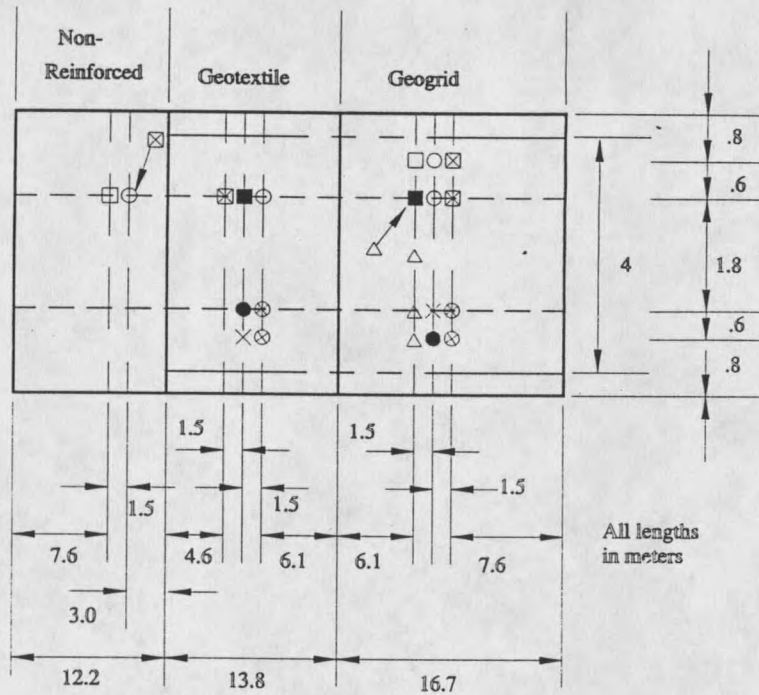


Figure 16. Roadway Instrumentation Layout

Table 3. Instrumentation Specifications

Instrument Location	Instrument Type	Gage Length mm	Strain Range (%)	Strain Sensitivity (%)
Geosyn.	VW Strain Gage	150	0.3	0.0001
Geosyn.	VW Displacement	280	9	0.009
Geosyn.	LVDT Displacement	50	+/- 10	+/- 0.03
Geosyn.	Foil Strain Gage	5	10	---
Base	VW Embedment Strain	161	0.3	0.0001
Base	VW Embedment Displ.	317	8	0.008
Base	LVDT Embed. Displ.	81	+/- 13	+/- 0.04
AC	VW Embed. Strain	153	0.3	0.0001

### Instrumentation Installation

Instruments Attached to the Geosynthetics. Instruments were installed by sandwiching the geosynthetic between the two mounting plates of the sensor and tightening the connecting bolts. Holes were predrilled in the geotextile to allow the bolts to pass through. A protective layer of medium sand, approximately 0.5 cm in thickness, was placed below each of the instruments attached to the geogrid. In addition, a small piece of the geotextile was placed above the footprint of the instrument to prevent the instrument from binding with the aggregate base course material. The protective layer of sand beneath the geogrid was continued along the length of the cables attached to the instruments and deepened to approximately 1 cm to prevent base course aggregate from puncturing the cables. The cables were also fastened to the geogrid ribs with plastic zip strips. The sand

pack was not used beneath the geotextile as it was with the geogrid.

Three strategies were employed for permanently covering and protecting the transducers located on the geosynthetics prior to the placement of base course aggregate. The first option consisted of covering the instrument with a half section of PVC pipe. The ends of the pipe were packed with sand to prevent base course from entering the pipe. The second option consisted of covering the transducer with medium sand and then covering the sand mound with a layer of geotextile. The third option consisted of covering the instrument with a medium sand and placing a half section of PVC pipe over the sand pack such that the entire pipe cavity was filled with sand. The options used for the instruments attached to the geosynthetics are listed in table 4. Due to limited number of vibrating wire displacement and strain gauges, not all cover options could be used for these sensors. Note that the PVC pipe used for instrument #1 was significantly more flexible than the other PVC pipes. All cables extending across the top surface of the geosynthetics were also covered with a sand pack to prevent cable damage from the aggregate base.

Due to the extensive environmental protection around the foil gauges, additional covering in the field consisted only of a thin layer of sand mounded atop the gauge locations. With the above precautions taken, the instruments on the geosynthetics were ready for the base course to be placed.

Instruments Embedded in Base Course. Prior to the placement of the aggregate base course, temporary covers were placed around the gauges to be embedded in the base to protect them from damage during compaction. Three types of covers were used to accommodate the different sizes of the instruments and to explore different methods. A large

Table 4. Geosynthetic Instrument Cover Options

Instrument Number	Geosynthetic Instrument Type	Cover Option
1	VW Displacement Gage	3
2	VW Displacement Gage	2
5	VW Strain Gage	1
9	VW Strain Gage	2
29	LVDT Displacement Gage	2
30	LVDT Displacement Gage	3
31	LVDT Displacement Gage	1
32	LVDT Displacement Gage	3

irrigation control box with the bottom removed was placed around the vibrating wire embedment displacement gauges. A layer of sand was placed in the bottom of the container and along the length of the cable extending from the container. A similar arrangement was used for the LVDT embedment gauges with a sand pack also being used. Both of these containers were rigid. A flexible tube was used to encase the vibrating wire embedment strain gauges. With these containers in place, base course material was placed and spread as previously described. Hand spreading was necessary in the vicinity of the embedment gauges.

Aggregate base was mounded around the outside of the two rigid containers such that the base course extended above the top of the container. This step was necessary to prevent the container from being pushed down by forthcoming compaction. The flexible container was allowed to extend above the base course grade such that the base course could be spread directly adjacent to the container. The flexibility of the container allowed for the compaction

equipment to compress both the container and the base as the compacter rolled over the location. Observing the compaction operation showed that both techniques work quite well and that no physical differences in the base course material existed between material adjacent to the containers and that lying far away.

Once the base course was compacted, the containers were pulled from the ground. The flexible container had to be slit to be removed while the other containers pulled from the ground more easily due to their sloped sides. Aggregate base material was then compacted around the instruments to backfill the cavities left by the containers. This was accomplished with the use of a short length of wooden stake and a hammer. The stake allowed for the base to be compacted well within areas interior to the discs of the gauges. The base was compacted to the greatest density possible. This technique also allowed for the gauges to be positioned within the middle of their range. This was accomplished by monitoring the instruments in real time while gently tapping the base course either in the interior or exterior areas of the end discs. The remaining base necessary to fill the cavity was placed in the same fashion. As described previously, additional base course was added to level the test section and additional compaction was provided. This compaction took place without any protection of the instruments.

Instruments Embedded in Asphalt Concrete. The embedment strain gauges in the asphalt concrete were placed using carrier blocks. This was accomplished by placing the gauge in an open wooden mold and compacting asphalt around the gauge with a wooden stake and hammer. For one of the gauges (# 10, over the geogrid under a wheel path), the

asphalt was allowed to cool and set-up over night. For the other three gauges, the asphalt was compacted approximately an hour before placement of the asphalt layer. These two approaches were taken to examine the effect of curing time on the compatibility of the carrier block with the surrounding AC. Using the carrier block compacted a day in advance, it was feared the AC constrained in the brick would not be sufficiently heated by the surrounding AC, with the result being that the block would not bond well with the adjacent material. It was speculated that this problem would be avoided by compacting the brick immediately before AC placement. The carrier blocks were oriented in the transverse direction of the roadway. The asphalt was placed as described previously with care taken to avoid driving over the gauges during the initial dumping of the asphalt.

### Wide Width Tension Testing

#### Loading Frame

The loading frame for in-air wide width tensile testing of geosynthetics consists of an upper and lower assembly. The frame is illustrated in figure 17. The loading frame accommodates a specimen with maximum dimensions of 1.8 m by 0.91 m. This size specimen is much larger than that used in most wide-width tensile tests, where specimens measure 200 mm by 100 mm. The large width is necessary to accommodate the different instruments placed on the specimen, while preserving a 2:1 ratio of specimen width to height. The 2:1 ratio is generally recommended to ensure that a condition of zero lateral strain is achieved over the majority of the central region of the specimen.

A modified roller grip system was used for the loading frame. The upper and lower

assemblies use 178 mm diameter steel cylinders which act as drums around which the geosynthetic is wrapped and gripped. The upper drum is rigidly attached to two vertical supports which connect to an I-beam which in turn rests on top of the load cell. The steel cylinder in the lower assembly contains a central axle, which it is rotated about during loading and unloading of specimens. The lower cylinder is attached to an I-beam via short vertical supports. The I-beam itself, is bolted to the bottom load platen of a Baldwin testing machine load frame. The Baldwin operates by driving the top load platen, and therefore the upper assembly, upwards.

The loading of a specimen is as follows. The geosynthetic is initially placed on the upper drum giving extreme attention to proper alignment. To prevent excessive slipping of the geosynthetic around the cylinder, a metal retaining strip measuring 20 mm by 5 mm in cross section is placed atop the leading edge of the geosynthetic and bolted to the cylinder. The bolt hole spacing is 10 cm. The geosynthetic is then wrapped around the cylinder  $2 \frac{1}{2}$  times such that the geosynthetic leaves the drum on the opposite side of the retaining strip. The geosynthetic is then wrapped a half-turn around the lower drum with a retaining strip fastening the specimen to the drum in the same manner as that used for the upper drum. The cylinder is then rotated to provide  $2 \frac{1}{2}$  wraps of specimen around the cylinder, with the cylinder then bolted to the vertical supports to prevent further rotation. The lower assembly is then moved by the Baldwin machine to remove slack in the specimen.

During loading of the specimen, the geosynthetic will slip a small amount around the drum. In addition, the material contained in the wrap will strain and deform. This makes it difficult to define a gauge length necessary to calculate an average strain for the specimen.

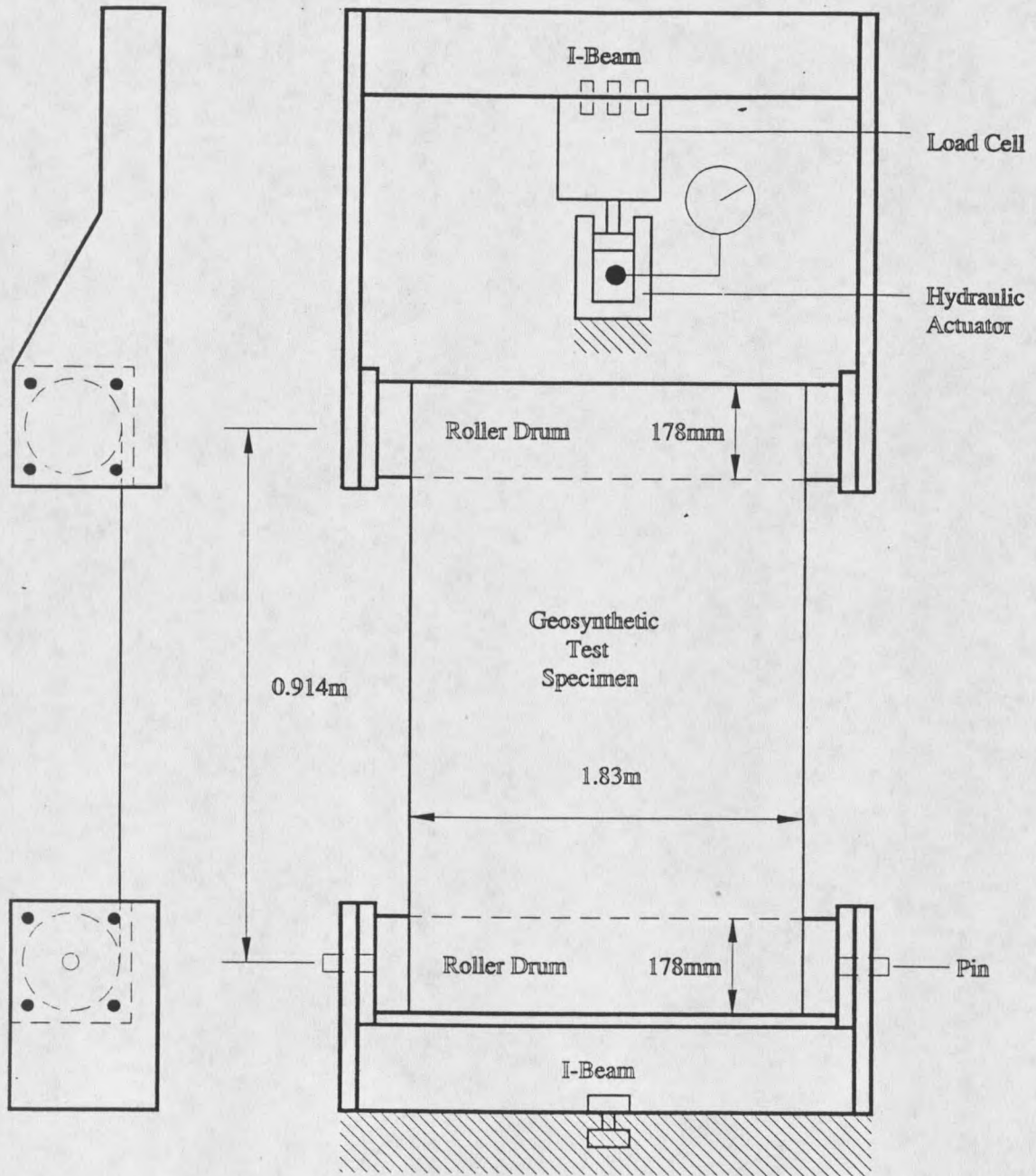


Figure 17. Schematic of Wide Width Tension Testing Frame

To overcome this problem, it was necessary to monitor the absolute displacement of two extreme points on the specimen, one close to the top of the specimen and one close to the bottom. This allowed the relative displacement between these two points to be calculated. Knowing the length between the two points allowed for the average strain across the specimen to be determined. This procedure was provided for two lateral positions along the specimen, such that the average strain could be determined along two vertical lines. Celesco (Canoga Park, CA) position transducers (PT-101) with a 25.4 cm range were used to monitor the absolute displacement of each of the four points. These transducers operate by a cable which extends from a spool within the transducer body. Additional cable was attached to this cable to allow for connections to the top of the specimen. The position transducers were clamped to the I-beam of the lower assembly. The mounts for the cable ends consisted of a bolt and washer arrangement with a cable attachment point being held as closely as possible to the face of the geotextile.

A Computer Boards (Mansfield, MA) data collection board (CIO-DAS08-PGM) was installed in a 386 PC with Computer Boards Control-CB software used to operate the board. A terminal board (CIO-MINI37) and 10V DC power supply were used to power and connect to the load cell and the four Celesco position transducers. The Control-CB software allowed for the data (as well as mathematically manipulated data) to be monitored and plotted real time on the screen of the PC. This feature was used to monitor the strain rate associated with the applied load during a test.

Several tests were performed on the geotextile and the geogrid with each material placed in both the machine and transverse directions while manually measuring the applied





























































































































































































































